HHS Public Access

Author manuscript

Sci Signal. Author manuscript; available in PMC 2020 August 02.

Published in final edited form as:

Sci Signal. ; 11(546): . doi:10.1126/scisignal.aar8371.

Oncogenic RAS isoforms show a hierarchical requirement for SOS2 to drive transformation

Erin Sheffels[1], **Nancy E. Sealover**[1], **Chenyue Wang**[1], **Do Hyung Kim**[1], **Isabella A. Vazirani**[1], **Elizabeth Lee**[1], **Elizabeth Tyrell**[2], **Deborah K. Morrison**[2], **Ji Luo**[3], **Robert L. Kortum**[1,*]

[1]Department of Pharmacology and Molecular Therapeutics, Uniformed Services University of the Health Sciences, Bethesda, MD 20814, USA.

[2]Laboratory of Cell and Developmental Signaling, NCI-Frederick, Frederick, MD 21702, USA.

[3]Laboratory of Cancer Biology and Genetics, Center for Cancer Research, National Cancer Institute, NIH, Bethesda, MD, USA.

Abstract

About a third of tumors harbor activating mutations in *HRAS, NRAS, or KRAS*, genes encoding guanine triphosphatases (GTPases) of the RAS family. In these tumors, wild-type RAS signaling cooperates with mutant RAS to promote downstream effector activation. This cooperation between wild-type and mutant RAS drives proliferation and transformation, suggesting that upstream activators of wild-type RAS are important modulators of mutant RAS-driven oncogenesis. Previous studies investigated the role of the guanine nucleotide exchange factor (GEF) SOS1 in KRAS-driven proliferation, but little is understood about the role of SOS2. Here, we found that RAS family members have a hierarchical requirement for SOS2 expression and activity to drive transformation. In *Sos2*$^{-/-}$ mouse embryonic fibroblasts, SOS2 critically mediated mutant KRAS-driven transformation, but was dispensable for transformation driven by HRAS. *Sos2* deletion reduced EGF-dependent wild-type HRAS activation and phosphorylation of the kinase AKT in cells expressing mutant RAS, and assays using pharmacological inhibition revealed a hierarchical requirement for signaling by the kinase PI3K in promoting RAS-driven transformation that mirrored the requirement for SOS2. KRAS-driven transformation required the GEF activity of SOS2 and was restored in *Sos2*$^{-/-}$ MEFs by expression of constitutively activated PI3K. Finally, CRISPR/Cas9-mediated deletion of *SOS2* reduced EGF-stimulated AKT phosphorylation and synergized with MEK inhibition to block transformation of *KRAS*-mutant tumor cells. These results indicate that SOS2-dependent PI3K signaling plays an important role in mutant KRAS-driven transformation; hence, SOS2 may be a therapeutic target in KRAS-driven cancers.

*Corresponding author. robert.kortum@usuhs.edu.

Author contributions: E.S. and R.L.K. designed the experiments and analyzed the data; E.S. and R.L.K. performed most of the experiments; N.E.S. performed spheroid assays and assisted in inhibitor treatment assays; C.W. assisted with focus forming and soft agar assays; D.H.K. assisted with CRISPR/Cas9 experiments; I.A.V. and E.L. performed promoter analysis for SOS2 protein abundance; E.T. and D.K.M. generated the mutant RAS constructs and prepared recombinant lentiviruses; J.L. helped with design of CRISPR experiments and generated the *KRAS* CRISPR sequences. E.S. and R.L.K. wrote the manuscript, and D.K.M. edited the manuscript.

Competing interests: The authors declare they have no competing interests.

Data and materials availability: All data needed to evaluate the conclusions in the paper are present in the paper or the Supplementary Materials. Raw data and materials are available upon request from R.L.K.

Additionally, our data reveal the importance of 3D-culture systems in investigating important mediators of mutant KRAS.

Introduction

The RAS family of small GTPases includes three genes, *HRAS, NRAS,* and *KRAS,* whose protein products (HRAS, NRAS, KRAS4A, and KRAS4B) are activated by multiple physiological inputs to regulate different cellular outcomes depending on the specific context, including proliferation, differentiation, growth, apoptosis, and cell survival (1, 2). RAS proteins are molecular switches that are active when they are GTP-bound and inactive when they are GDP-bound. They are activated by RAS Guanine Nucleotide Exchange Factors (RASGEFs) that exchange GDP for GTP on RAS, and are inactivated by their own intrinsic GTPase activity, which is facilitated by RASGTPase-activating proteins (RASGAPs). Receptor tyrosine kinase (RTK) engagement recruits the RASGEFs Son of Sevenless 1 and 2 (SOS1 and SOS2) to the plasma membrane, where they induce nucleotide exchange and activate RAS. Active RAS then signals via multiple effectors to initiate downstream signaling cascades important for proliferation and survival, including the Raf/MEK/ERK kinase cascade and the PI3K/AKT pathway.

In addition to the role of RAS in RTK-dependent signaling, somatic mutations in *HRAS*, *NRAS*, or *KRAS* drive oncogenesis in approximately 30% of human tumors. These oncogenic *RAS* mutations, which most commonly cause amino acid substitutions at codons 12, 13, or 61, impair RASGAP-mediated GTP hydrolysis leading to constitutive GTP binding and activation. While this constitutive RAS activation was originally thought to make *RAS* mutant tumors independent of upstream signaling, we now know that activation of non-mutated wild-type RAS plays an important role in modulating downstream effector signaling during mutant RAS-driven tumorigenesis. The wild-type allele of the corresponding mutated *RAS* isoform is frequently deleted in RAS-driven tumors, suggesting that it may have a tumor suppressor role (3–5). This hypothesis is supported by observations in vitro (6) and in vivo with mouse models (7, 8). In contrast, the other two non-mutated wild-type RAS family members are necessary for mutant RAS-driven proliferation and transformation in some contexts (9–12). The wild-type RAS isoforms potentially contribute through their ability to activate effector pathways that the mutant isoform does not strongly activate, making the cellular outcome a product of signaling by wild-type and mutant RAS (13).

Two models have been proposed to explain how wild-type RAS signaling cooperates with mutant RAS to promote downstream effector activation and RAS-driven oncogenesis. In the first model, RTK-dependent activation of wild-type RAS supplements the basal oncogenic signaling from mutant RAS to fully activate downstream effector pathways and promote proliferation in *RAS* mutant tumor cell lines (11, 14, 15). In the second model, mutant RAS^{GTP} binds an allosteric pocket on the RASGEF SOS1 that relieves SOS1 autoinhibition, increasing its catalytic activity up to 80-fold (16). Relief of SOS1 autoinhibition then sets up a RAS^{GTP}–SOS1–wild-type RAS positive feedback loop that enhances activation of

downstream effectors and is important for proliferation of *KRAS* mutant pancreatic cancer cells (17).

While a role for SOS1 in *KRAS* mutant pancreatic cancer proliferation has been established, a role for SOS2 in mutant *RAS* driven oncogenesis has not been investigated. Here, we use immortalized *Sos2*$^{-/-}$ mouse embryo fibroblasts (MEFs) to determine the role of SOS2 in H-, N-, and KRAS-driven transformation. We found that there was a hierarchal requirement for SOS2 in RAS-driven transformation (KRAS > NRAS > HRAS), with KRAS being the most SOS2-dependent RAS isoform. Using mutated SOS2 constructs, we found that KRAS-driven transformation was dependent on SOS2 RASGEF activity, but not on putative SOS2 allosteric activation. SOS2 was required for EGF-stimulated, but not basal, wild-type HRAS activation in cells expressing mutant KRAS. At the level of effector signaling, *Sos2* deletion reduced RTK-dependent AKT phosphorylation in cells expressing all mutant RAS isoforms. However, we also found that there was a hierarchical requirement for PI3K signaling in promoting RAS-driven transformation (KRAS ≥ NRAS > HRAS) that mirrored the hierarchical requirement for SOS2. Furthermore, KRAS-driven transformation could be rescued in *Sos2*$^{-/-}$ MEFs by introduction of an activated PI3K catalytic subunit. Finally, deletion of *SOS2* reduced RTK-dependent AKT phosphorylation and synergized with the MEK inhibitor trametinib to block transformation of *KRAS*-mutant tumor cell lines. These results indicate that SOS2-dependent PI3K signaling plays an important role in mutant KRAS-driven transformation, and that SOS2 may be a therapeutic target in KRAS-driven cancers. Additionally, the specific requirement for SOS2 to promote mutant KRAS-driven proliferation in 3D, but not 2D, culture suggests that anchorage-independent screens must be used to supplement current 2D screening efforts when investigating therapeutic interventions to treat *KRAS* mutant tumors.

Results

Mutant RAS isoforms show a hierarchical requirement for Sos2 to drive transformation

Previous work has shown that activation of wild-type RAS promotes mutant RAS-dependent oncogenesis by at least two mechanisms. First, RTK-dependent wild-type RAS activation, presumably via the RASGEFs SOS1 and/or SOS2, cooperates with mutant H-, N-, and KRAS to promote RAS effector activation and cancer cell proliferation (11, 15). Second, mutant KRAS allosterically activates SOS1 (16), generating a $KRAS^{GTP}$–SOS1–wild-type RAS feedback loop that is required for proliferation of pancreatic cancer cells (17). While this contribution of SOS1 in mutant *KRAS*-driven cancer cell proliferation has been established, the specific role of SOS2 in *RAS* mutated tumors is not yet clear.

Previous work has shown a role for SOS1, but not SOS2, in anchorage-dependent (2D) proliferation in primary MEFs (18); however, we wanted to specifically assess the role of SOS2 in mutant RAS-dependent transformation. Since primary MEFs require cooperating oncogenes in addition to mutant RAS to promote transformation (19), we first generated immortalized MEFs which can be transformed by mutant RAS alone (20). To establish a model system to allow us to examine the specific role of SOS2 in oncogenic transformation, we immortalized *Sos1*$^{f/f}$ and *Sos1*$^{f/f}$*Sos2*$^{-/-}$ MEFs by a 3T6 protocol (21, 22) to generate stable cell lines (hereafter referred to as *Sos2*$^{+/+}$ and *Sos2*$^{-/-}$ MEFs). To assess the role of

SOS2 in mutant RAS-driven proliferation and transformation, we then stably expressed HA-tagged $HRAS^{G12V}$, $NRAS^{G12V}$, or $KRAS4B^{G12V}$ (hereafter referred to as $KRAS^{G12V}$) in the *Sos2*$^{+/+}$ and *Sos2*$^{-/-}$ MEFs at 0.2–3 times total endogenous RAS protein abundance (Fig. 1A). While neither *Sos2* deletion nor mutant RAS expression altered SOS1 protein abundance, expression of mutant RAS family members did decrease expression of EGFR to different extents, potentially due to feedback regulation on the signaling pathway (Fig. 1A).

As expected, expression of oncogenic H-, N-, or $KRAS^{G12V}$ enhanced cell proliferation over vector controls in immortalized MEFs (fig. S1); *Sos2* deletion did not affect GTP loading of the mutant RAS protein (Fig. 1A), did not alter proliferation driven by mutant NRAS or KRAS, and only modestly reduced proliferation by driven mutant HRAS on the last day of a 5-day growth curve (Fig. 1B and fig. S1). These data suggest that SOS2 is not a critical mediator of mutant KRAS or NRAS-driven proliferation and has a minimal effect on proliferation driven by HRAS, in agreement with a previous study in primary MEFs showing that SOS1, but not SOS2, is a critical mediator of proliferation (18). To assess RAS-driven transformation we examined two common features of transformed cells: anchorage-independent growth (soft agar assay, Fig. 1C) and loss of contact inhibition (focus-forming assay, Fig. 1D). The effect of *Sos2* deletion on RAS-driven transformation differed depending on which mutant RAS isoform was expressed. *Sos2* deletion did not affect $HRAS^{G12V}$-induced anchorage-independent growth (Fig. 1C), loss of contact inhibition (Fig. 1D), or morphologic transformation (Fig. 1E), indicating that SOS2 was dispensable for $HRAS^{G12V}$–induced transformation. In contrast, *Sos2* deletion reduced the transforming capacity of $NRAS^{G12V}$ and critically mediated transformation driven by $KRAS^{G12V}$ (Fig. 1C–E). *Sos2*$^{-/-}$ MEFs expressing $NRAS^{G12V}$ showed a 50% reduction in colony formation in soft agar (Fig. 1C) and qualitatively reduced the proportion of cells showing loss-or-contact inhibition (Fig. 1D), indicating that SOS2 promoted, but was not required for, transformation by $NRAS^{G12V}$. *Sos2*$^{-/-}$ MEFs expressing $KRAS^{G12V}$ exhibited minimal anchorage-independent growth (Fig. 1C), remained contact inhibited (Fig. 1D), and did not show any signs of morphologic transformation (Fig. 1E). These data suggest that there is a hierarchical requirement for SOS2 in mutant RAS-driven transformation.

Within the pool of *RAS*-mutant tumors, *KRAS* is the most frequently mutated RAS family member (85%). Most *KRAS* mutations occur at codons G12, G13, or Q61, with the frequency of specific mutations varying depending on the tumor type (23, 24). Since our data indicated that *Sos2* deletion has a larger effect on transformation driven by mutant KRAS compared to mutant H- or NRAS, we further investigated the requirement of SOS2 in mutant KRAS-driven transformation. To determine whether this requirement is mutation-specific, we expressed either wild-type KRAS or one of six common KRAS oncogenic mutants (G12C, G12D, G12V, G13D, Q61L, or Q61R) in *Sos2*$^{+/+}$ and *Sos2*$^{-/-}$ MEFs (Fig. 2A). For all KRAS G12 and G13 oncogenic mutants examined, SOS2 critically mediated mutant KRAS-induced anchorage-independent growth (Fig. 2B) and loss of contact inhibition (Fig. 2C). In contrast, for the KRAS Q61 mutants, low levels of KRAS-induced loss of contact inhibition were detectable in the absence of SOS2, indicating that while Q61 mutants require SOS2 for full transformation, they can induce low levels of transformation without SOS2 present. These data suggest that SOS2 is required for full KRAS-driven

transformation in MEFs, regardless of the specific KRAS oncogenic mutation, and that it is particularly required for transformation driven by G12 and G13 mutations.

SOS2 RASGEF activity is required for KRAS-driven transformation

KRAS Q61 mutants have lower levels of GTPase activity than the already reduced levels in G12 and G13 mutants, potentially making them less dependent on GEF activity to restore GTP binding (25). Because of this, we first assessed whether KRAS GTP loading was dependent on SOS2 for $KRAS^{G12C}$, $KRAS^{G12V}$, and $KRAS^{Q61R}$ mutant proteins. We did not observe any significant alterations in $KRAS^{GTP}$ abundance upon *Sos2* deletion for any of the mutant KRAS proteins (fig. S2), indicating that the activation of mutant KRAS is not dependent on SOS2.

Next, we examined the mechanism by which SOS2 contributes to KRAS-driven transformation by restoring SOS2 expression in $Sos2^{-/-}$ MEFs, using either wild-type or mutated SOS2 constructs to distinguish the relative contributions of RTK−SOS2−wild-type RAS and $KRAS^{GTP}$−SOS2−wild-type RAS signaling. However, due to the hypothesized dynamics of SOS signaling, we first created a construct that would allow us to restore SOS2 in $Sos2^{-/-}$ MEFs at near endogenous ($Sos2^{+/+}$) protein abundance. In a quantitative proteomic analysis of the core components in the RTK/RAS/MAPK signaling pathway, Shi et al. (26) showed that the absolute abundance of SOS1 and SOS2 are extremely low relative to the other core proteins in the RTK/RAS signaling pathway, leading them to hypothesize that SOS1 and SOS2 may be ‘stoichiometric bottlenecks’ for signal transduction through this pathway. Their findings suggest that exogenous introduction of SOS2 at super-physiologic protein abundance could result in aberrant RAS-dependent signaling, making rescue experiments difficult to interpret. To circumvent this, *SOS2* was cloned into lentiviral vectors containing one of five different promoters, each with different predicted expression levels, and then stably expressed in $Sos2^{-/-}$ MEFs (fig. S3A). The high activity EF1α and UbC promoters, and the moderate activity PGK promotor, lead to SOS2 protein abundance >30-fold and 18-fold higher than endogenous SOS2 found in $Sos2^{+/+}$ MEFs, respectively, indicating that these promoters are not optimal for expressing SOS2 at physiologic protein abundances. In contrast, using either an SV40 or a minimal CMV (mCMV) promoter to drive *SOS2* expression lead to SOS2 abundance at only 2–5-fold above that of endogenous SOS2. This near-endogenous SOS2 abundance restored transformation in $Sos2^{-/-}$ MEFs expressing $KRAS^{G12V}$ (fig. S3B). Since the SV40 promoter gave more consistent near-endogenous SOS2 abundance across multiple experiments, we used this promoter for subsequent SOS2 rescue experiments.

Bentley et al (15) previously showed that wild-type N- and HRAS are required for transformation of KRAS mutant cancer cells. We hypothesized that SOS2 potentially promotes KRAS driven transformation by one of two mechanisms: either by RTK-dependent activation of downstream effectors, or as a part of an allosteric $KRAS^{GTP}$−SOS2−wild-type RAS feedback loop similar to the one previously described for SOS1 (16, 17). To differentiate between these two possibilities, we made constructs with point mutations in *SOS2* that are homologous to mutations previously identified in *SOS1*: $SOS2^{F927A}$, which is homologous to the $SOS1^{F929A}$ mutant that ablates RASGEF activity (27); and $SOS2^{W727E}$,

which is homologous to the SOS1^{W729E} mutant that renders SOS1 unable to be allosterically activated by RAS^{GTP} (16, 28). If the major contribution of SOS2 is to promote RTK −SOS2−wild-type RAS signaling, then only the SOS2^{F927A} mutant will fail to restore transformation in *Sos2*$^{-/-}$ MEFs expressing mutant KRAS. In contrast, if KRAS^{GTP} −SOS2−wild-type RAS signaling is important for mutant KRAS-driven transformation, then neither the SOS2^{F927A} nor the SOS2^{W727E} mutants will restore transformation in *Sos2*$^{-/-}$ MEFs expressing mutant KRAS (Fig. 3A).

We stably introduced wild-type SOS2, SOS2^{F927A}, or SOS2^{W727E} into in *Sos2*$^{-/-}$ MEFs expressing KRAS^{G12C}, KRAS^{G12V}, or KRAS^{Q61R} (Fig. 3B). Wild-type SOS2 restored KRAS-driven anchorage independent growth (Fig. 3C), loss of contact inhibition (Fig. 3D), and morphologic transformation (Fig. 3E) in *Sos2*$^{-/-}$ MEFs expressing each of the mutant RAS constructs. In contrast, RASGEF-dead SOS2 (SOS2^{F927A}) could not restore KRAS-driven transformation in cells expressing either KRAS^{G12C} or KRAS^{G12V} (Fig. 3C–E). In cells expressing KRAS^{Q61R}, however, we observed that SOS2^{F927A} enhanced the low level of transformation we had observed in *Sos2*$^{-/-}$ MEFs expressing KRAS^{Q61R}, suggesting that although SOS2 did not alter the global GTP loading of KRAS^{Q61R}, the GTPase activity of different oncogenic KRAS mutants may modulate their dependence on SOS2. However, while KRAS^{Q61R} exhibited lower dependence on SOS2 for transformation than either KRAS^{G12C} or KRAS^{G12V}, SOS2 GEF activity was still required for full KRAS^{Q61R}-driven transformation. On the other hand, a SOS2 mutant construct resistant to RAS^{GTP}-dependent feedback activation (SOS2^{W727E}) restored KRAS-driven transformation similarly to wild-type SOS2. Since SOS2 RASGEF activity, but not allosteric RAS^{GTP}-dependent SOS2 activation, was required for mutant KRAS to fully transform MEFs, these data suggest that RTK-dependent SOS2 signaling to wild-type RAS cooperates with basal signaling from mutant KRAS to promote the transformed phenotype.

To directly examine the role of SOS2 in activation of wild-type RAS, we expressed V5-tagged wild-type HRAS in *Sos2*$^{+/+}$ and *Sos2*$^{-/-}$ MEFs expressing HA-KRAS^{G12C} and performed GST-RBD pulldowns to directly assess HRAS^{GTP} in both actively cycling cells and upon EGF stimulation after an overnight starve (Fig. 3F). Activation of wild type HRAS was significantly decreased in actively cycling *Sos2*$^{-/-}$ MEFs compared to the *Sos2*$^{+/+}$ MEFs, indicating that SOS2 is important for full wild-type HRAS activation (Fig. 3F, left). In serum starved cells, the abundance of HRAS^{GTP} was unchanged upon *Sos2* deletion, indicating that basal KRAS^{G12C}-dependent activation of wild-type HRAS was independent of SOS2. EGF-stimulation after an overnight starve showed increased wild-type HRAS activation in *Sos2*$^{+/+}$ MEFs, but not *Sos2*$^{-/-}$ MEFs, suggesting that SOS2-dependent activation of wild-type HRAS is downstream of RTK signaling in cells with mutant KRAS (Fig. 3F, right). Furthermore, assessment of V5-HRAS activation in KRAS^{G12C} *Sos2*$^{-/-}$ MEFs expressing wild-type SOS2, SOS2^{F927A}, or SOS2^{W727E} showed that activation of wild-type HRAS was increased in *Sos2*$^{-/-}$ MEFs expressing wild-type SOS2 and SOS2^{W727E} compared to either vector controls or *Sos2*$^{-/-}$ MEFs expressing SOS2^{F927A} (Fig. 3G). These data indicate that SOS2 GEF activity, but not allosteric feedback activation of SOS2 by oncogenic KRAS, is key to SOS2-dependent activation of wild-type HRAS downstream of RTKs.

SOS2 promotes EGF-stimulated AKT phosphorylation in cells expressing mutant RAS

The data presented in Fig. 3 suggest that RTK-SOS2 signaling through wild-type RAS to downstream Raf/MEK/ERK and PI3K/AKT effector pathways augments basal $KRAS^{G12V}$ signaling to promote oncogenic transformation. To test this possibility, we assessed EGF-stimulated phosphorylation of ERK and AKT in *Sos2*$^{+/+}$ and *Sos2*$^{-/-}$ MEFs expressing each RAS^{G12V} isoform (Fig. 4). Although mutant RAS expression reduced EGFR expression (Fig. 1A), *Sos2* deletion did not have any further effects on EGFR protein abundance, so comparisons of EGF-stimulated signaling in *Sos2*$^{+/+}$ or *Sos2*$^{-/-}$ MEFs expressing any individual mutant RAS isoform were not confounded by alterations in EGFR abundance (Fig. 4A). *Sos2* deletion did not significantly alter EGF-stimulated ERK phosphorylation in cells expressing mutant H-, N-, or KRAS, as both peak ERK phosphorylation and prolonged Raf/MEK/ERK signaling were not significantly reduced by *Sos2* deletion (Fig. 4A, B). In contrast, *Sos2* deletion significantly reduced EGF-stimulated AKT phosphorylation in cells expressing mutant H-, N-, or KRAS (Fig. 4A, B). Loss of SOS2 reduced peak AKT phosphorylation and blocked prolonged PI3K/AKT signaling. These data suggest that SOS2 is important for RTK-stimulated PI3K/AKT, but not Raf/MEK/ERK, signaling. However, these data do not sufficiently explain the differential requirement for SOS2 in RAS isoform-driven transformation, since the reduction in AKT phosphorylation was similar in cells expressing each of the mutant RAS isoforms.

Mutant RAS isoforms show a differential requirement for PI3K for transformation

To reconcile the hierarchical effect of *Sos2* deletion on mutant RAS-dependent transformation with the equivalent decrease in RTK-stimulated AKT phosphorylation, we examined whether MEFs expressing each mutant RAS isoform showed differential sensitivity to PI3K/AKT or Raf/MEK/ERK effector pathway inhibition. Since our initial observation showed that *Sos2* deletion altered transformation but not proliferation, we assessed effector pathway inhibition under both anchorage-dependent and anchorage-independent (transforming) conditions. *Sos2*$^{+/+}$ MEFs expressing H-, N-, or $KRAS^{G12V}$ were seeded on cell-culture treated (anchorage-dependent) and ultra-low attachment (anchorage-independent) 96-well plates and treated with increasing doses of the PI3K inhibitor LY294002 (Fig. 5A), the AKT inhibitor AZD5363 (Fig. 5B), or the MEK inhibitor trametinib (Fig. 5C). We confirmed that these inhibitors blocked signaling downstream of their intended target by comparing the phosphorylation of downstream targets in treated and untreated MEFs (fig. S4). We then assessed two measurements of drug potency: the IC_{50}, which measures the drug concentration at half maximal inhibition, and the area under the viability curve (AUC), which takes into account both the potency and total level of growth inhibition by a given compound. Cells expressing the different mutant RAS isoforms did not show any differences in their responses to PI3K, AKT, or MEK inhibition under anchorage-dependent growth conditions (Fig. 5A–C, left). These data suggest that mutant H-, N-, and KRAS-driven anchorage-dependent proliferation depends on these RAS effector pathways to a similar extent.

In contrast to the equivalent effects of effector pathway inhibition on mutant RAS-driven anchorage-dependent growth, RAS-expressing cells showed a hierarchical requirement for PI3K (Fig. 5A, right) to promote anchorage-independent growth, mirroring the requirement

for SOS2, with KRAS ≥ NRAS > HRAS. When mutant RAS-expressing MEFs were treated with increasing concentrations of LY294002, anchorage-independent proliferation was inhibited at lower drug concentrations in $KRAS^{G12V}$ expressing MEFs compared to $HRAS^{G12V}$ expressing MEFs, with a significant shift in the dose response curve to lower drug concentrations, resulting in significant decrease in the AUC and a 5-fold decrease in the IC_{50} for LY294002 (Fig. 5A). Furthermore, $NRAS^{G12V}$ expressing MEFs showing an intermediate phenotype between MEFs expressing the other two RAS family members. $NRAS^{G12V}$ expressing MEFs showed a 2-fold decrease in the IC_{50} for LY294002 but no difference in the AUC compared to $HRAS^{G12V}$ expressing MEFs.

To confirm that these differences were due to inhibition of the PI3K/AKT pathway and not off-target effects of LY294002, RAS ^{G12V}-expressing MEFs were treated with the AKT inhibitor AZD5363 (Fig. 5B). Similar to what was observed for PI3K inhibition, RAS-isoform expressing MEFs showed a differential requirement for AKT to promote anchorage-independent growth, with KRAS = NRAS > HRAS. Here again, $KRAS^{G12V}$ expressing MEFs showed a decrease in the AUC and a 5-fold decrease in the IC_{50} for the AKT inhibitor AZD5363 compared to $HRAS^{G12V}$ expressing MEFs. However, unlike the intermediate phenotype the $NRAS^{G12V}$ expressing cells showed for PI3K inhibition, $NRAS^{G12V}$ expressing MEFs were as sensitive to AKT inhibition as $KRAS^{G12V}$ expressing cells.

In contrast to the increased sensitivity of $KRAS^{G12V}$–expressing cells to PI3K/AKT inhibition, treatment of mutant RAS-expressing MEFs with the MEK inhibitor trametinib revealed that $HRAS^{G12V}$-expressing MEFs were more sensitive to MEK inhibition compared to either N- or $KRAS^{G12V}$-expressing MEFs. $HRAS^{G12V}$-expressing MEFs showed a 2-fold decrease in the IC_{50} for trametinib compared to N- and $KRAS^{G12V}$-expressing MEFs. These data suggest that mutant HRAS may have a slightly increased requirement for Raf/MEK/ERK signaling to drive transformation compared to mutant N- or KRAS expressing cells. (Fig. 5C).

To further examine the role of PI3K in mutant RAS-isoform driven transformation, we assessed cancer spheroid formation in $Sos2^{+/+}$ MEFs expressing H-, N- or $KRAS^{G12V}$ treated with increasing doses of LY294002 (Fig. 5D). Cells were seeded in 96-well ultra-low attachment round-bottomed plates, and imaged 16 hours after plating (Day 0) and again seven days later. In untreated cells, spheroid size increased in all RAS^{G12V}-expressing MEFs over the 7-day period but not in vector controls (Fig. 5D), indicating the RAS^{G12V} can induce cancer spheroid growth in MEFs. Mutant RAS-dependent spheroid growth showed the same hierarchical dependence on SOS2 that had been observed in other transformation assays (Fig. 5D, right and fig. S5). Furthermore, when we assessed the effects of LY294002 treatment on cancer spheroid growth in $Sos2^{+/+}$ MEFs, we observed a similar hierarchical requirement for PI3K signaling to the one observed in the anchorage-independent proliferation assay, with KRAS > NRAS > HRAS. The LY294002 concentration that inhibited spheroid growth for each mutant RAS isoform corresponded to the IC_{50} value we observed for inhibiting anchorage-independent proliferation. These data further support the existence of a hierarchical requirement for PI3K signaling to promote RAS-driven transformation that correlates with the requirement for SOS2 expression.

Activated PI3K rescues KRAS-driven transformation in Sos2$^{-/-}$ MEFs

The data presented up to this point suggest that RTK−SOS2-dependent PI3K signaling is required for mutant KRAS-induced transformation in MEFs. To determine if restoring PI3K/AKT signaling is sufficient to restore mutant KRAS-dependent transformation in *Sos2*$^{-/-}$ MEFs, we expressed an activated form of the p110α catalytic subunit (p110α^{H1047R}) at near-endogenous levels, alone or in combination with KRAS^{G12V}, in *Sos2*$^{+/+}$ and *Sos2*$^{-/-}$ MEFs (Fig. 6A). We then assessed transformation using focus forming assays (Fig. 6B, C) and by assessing morphologic transformation (fig. S6). Expression of activated p110α^{H1047R} alone modestly transformed *Sos2*$^{+/+}$ MEFs as previously reported (29). This p110α^{H1047R}-driven transformation was unaffected by *Sos2* deletion (Fig. 6B), suggesting that PI3K is downstream of, or parallel to, SOS2 in these cells. KRAS^{G12V} robustly transformed immortalized *Sos2*$^{+/+}$ MEFs (Fig. 6B), and this transformation was further enhanced by combining p110α^{H1047R} with KRAS^{G12V} (Fig. 6B,C), confirming previous reports of synergic transformation between KRAS^{G12V} and either p110α (30) or AKT (31). As shown previously, KRAS^{G12V} was unable to transform *Sos2*$^{-/-}$ MEFs alone (Fig. 1 and 6B, C). In contrast, combined p110α^{H1047R} and KRAS^{G12V} expression robustly transformed *Sos2*$^{-/-}$ MEFs similar to the transformation observed in *Sos2*$^{+/+}$ MEFs (Fig. 6B). These data suggest that constitutively activated PI3K can substitute for SOS2 to promote KRAS-driven transformation.

SOS2 promotes transformation of KRAS-mutant tumor cells

We next tested whether the requirement of *Sos2* for mutant KRAS-driven transformation in MEFs could be replicated in *KRAS* mutant human tumor cells. Since transformation assays typically grow for 2–4 weeks, we used CRISPR/Cas9 to delete *SOS2* rather than using a transient siRNA approach. We cloned several candidate sgRNAs that were previously used to target *SOS2* in a genome-wide CRISPR/Cas9 screen (32) into the lentiCRISPRv2 vector, which allows for simultaneous expression of the sgRNA and Cas9 (33). Lentiviruses were then produced from these constructs and used to evaluate the efficiency of *SOS2* deletion by each sgRNA in 293T cells. We found seven different sgRNAs that deleted *SOS2* in >80% of 293T cells (fig. S7). Three of these sgRNAs that target non-overlapping regions of *SOS2* (#1, #9, and #16) were selected and used to examine the role of SOS2 in transformation *KRAS* (G12V) mutant YAPC pancreatic cancer cells.

YAPC cells were infected with either a non-targeting sgRNA (NT), an sgRNA targeting *KRAS*, or one of three sgRNAs targeting *SOS2* (#1, #9, or #16). The resulting cells were then selected for 10 days post-infection to allow for CRISPR/Cas9-mediated gene deletion. The effect of *SOS2* deletion was examined in pooled cultures to avoid any effects of clonal selection. *KRAS* sgRNA expression reduced KRAS abundance by >95%, and each *SOS2* sgRNA reduced SOS2 protein abundance by >80% compared to NT controls, indicating that *SOS2* had been deleted in at least 80% of cells (Fig. 7A). *KRAS* deletion completely inhibited anchorage-independent growth of YAPC pancreatic cancer cells, confirming the KRAS dependence of this cell line. Each of the three *SOS2* sgRNAs reduced the number of transformed colonies by >70%, and the colonies that did form were generally smaller than the colonies in NT controls. These data suggest that SOS2 is required for full mutant KRAS-driven oncogenic transformation in *KRAS* mutant pancreatic cancer cells.

To test whether the requirement for SOS2 to promote mutant KRAS-driven transformation might hold true in a *KRAS* mutant tumor cell line from another anatomical site, we assessed whether SOS2 was required for transformation in *KRAS* (G12C) mutant H358 lung cancer cells. These cells have been used to show the specificity of covalent $KRAS^{G12C}$-specific inhibitors, and are highly dependent on KRAS signaling for proliferation and transformation (34). Similar to what we observed in YAPC cells, *KRAS* deletion inhibited cancer spheroid growth in H358 lung cancer cells (Fig. 7B). Furthermore, deletion of *SOS2* using two different sgRNAs blocked spheroid growth to a similar extent as deleting *KRAS* itself. These data suggest that SOS2 is an important modulator of mutant KRAS-driven transformation in human tumor cells from multiple anatomic sites.

To determine whether the mechanism of SOS2-dependence in *KRAS* mutant cancer cells may be similar to the mechanism in mutant KRAS-expressing MEFs, we tested the activation of the Raf/MEK/ERK and the PI3K/AKT pathways in YAPC pancreatic cancer cells after deletion of *SOS2*. Deletion of *SOS2* with any of the three sgRNAs (#1, #9, or #16) had no effect on ERK phosphorylation in actively cycling cells (Fig. 7C), or after EGF stimulation (Fig. 7D). These data suggest that, similar to our assessment of the role of *Sos2* in MEFs, deletion of *SOS2* alone does not alter EGF-dependent ERK phosphorylation in *KRAS* mutant cancer cells. In contrast, deletion of *SOS2* significantly decreased AKT phosphorylation in actively cycling cells (Fig. 7C) and after EGF stimulation (Fig. 7D). These data indicate that, similar to the mechanism we had observed in $Sos2^{-/-}$ MEFs, SOS2 is required for full RTK-stimulated AKT phosphorylation in a *KRAS* mutant cancer cell line.

With the notable exception of covalent KRAS G12C-specific inhibitors (34), single agent approaches have been broadly unsuccessful in limiting growth of *KRAS* mutant tumors. In contrast, combined inhibition of KRAS effector pathways, such as the combination of MEK and PI3K inhibitors, has shown marked benefit over single agents alone (35–37). Since *SOS2* deletion reduced AKT phosphorylation in *KRAS* mutant pancreatic cancer cells (Fig. 7C–D), we hypothesized that *SOS2* deletion might act similarly to a PI3K inhibitor and synergize with MEK inhibition to block proliferation and transformation in *KRAS* mutant tumor cells. To understand whether *SOS2* deletion would alter the response of *KRAS* mutant tumor cells to effector pathway inhibition, we assessed the combination of either *SOS2* or *KRAS* deletion with either the PI3K inhibitor buparlisib (Fig. 8A,B) or the MEK inhibitor trametinib (Fig. 8C,D) under both anchorage-dependent and anchorage-independent (transforming) conditions. We confirmed that these inhibitors blocked signaling downstream of their intended target by comparing the phosphorylation of downstream targets in treated and untreated YAPC cells (fig. S8). Deletion of *SOS2* had no significant effect on the IC_{50} of buparlisib in either YAPC cells (Fig. 8A) or H358 cells (Fig. 8B), consistent with the idea that *SOS2* deletion and buparlisib treatment both act on the PI3K pathway. While *SOS2* deletion did significantly decrease the area under the curve (AUC), especially under anchorage-independent conditions (Fig. 8A–B, right), this decrease was due to a decrease in the overall cell number after 5 days in culture in cells with *SOS2* deleted (see untreated cells). In contrast, we observed a synergistic effect between *SOS2* deletion and trametinib treatment in inhibiting both anchorage-dependent and anchorage-independent growth. *SOS2* deletion reduced the IC_{50} for trametinib by 2–3-fold under anchorage-dependent conditions

(Fig. 8C–D, left) and 5-fold under anchorage-independent growth conditions (Fig. 8C–D, right).

To determine if *SOS2* deletion had a similar effect to PI3K inhibition in synergizing with trametinib to block *KRAS* mutant tumor cell growth, YAPC or H358 cells expressing a non-targeting sgRNA were treated with 100 nM buparlisib, a dose just below the threshold for inhibiting cell growth with buparlisib alone (Fig. 8A–B, red arrows), in combination with trametinib. The effect of combining trametinib with low dose buparlisib were similar to the effects of combining trametinib with *SOS2* deletion (Fig. 8C–D, compare red and blue curves). These data indicate that, similar to PI3K inhibition, *SOS2* deletion can synergize with MEK inhibition to block proliferation and transformation of *KRAS* mutant tumor cell lines. Further, these data suggest that SOS2 is an unappreciated therapeutic target for the treatment of *KRAS* mutant tumors.

Discussion

Driver mutations in the RAS family of GTPases occur in ~30% of human tumors (38, 39). Although these tumors were originally thought to proliferate independently of upstream signaling inputs, we now know that signaling through wild-type RAS cooperates with mutant RAS to activate downstream effector pathways and drive oncogenic proliferation (12). Here, we demonstrated that there is a hierarchical requirement for the RASGEF SOS2 in RAS isoform-driven transformation, with KRAS > NRAS > HRAS. This requirement for SOS2 parallels a differential requirement for PI3K signaling to maintain the RAS-transformed phenotype, and in doing so, reveals a previously unappreciated RTK-SOS2-RAS-PI3K signaling pathway that supplements mutant KRAS-driven PI3K activation to drive oncogenic transformation.

Why is wild-type RAS signaling required for mutant RAS-driven proliferation and transformation?

Mutant H-, N-, and KRAS can all interact with the major RAS effectors PI3K and Raf, thereby constitutively activating the PI3K/AKT and Raf/MEK/ERK pathways. Why, then, would wild-type RAS signaling be required to cooperate with mutant RAS to promote proliferation and oncogenic transformation? Though RAS isoforms interact with the same signaling effectors, they activate these effectors to different extents (40, 41), which are not correlated with a difference in binding affinity (42) or isoform stability (43). A potential role, then, for wild-type RAS is to activate the effector pathways that mutant RAS does not strongly activate, making the cellular outcome a product of signaling by wild-type and mutant RAS (13). For RAS-dependent activation of Raf and PI3K, multiple groups have shown an inverse relationship in the ability of mutant RAS isoforms to activate these effectors: mutant HRAS is a potent activator of PI3K but a poor activator of Raf, and conversely KRAS potently activates Raf but poorly activates PI3K (31, 40, 41). In fact, in *KRAS* mutant colon cancer cells, ERK signaling is mutant KRAS-dependent, but PI3K signaling is mutant KRAS-independent, and instead depends on RTK signaling for activation (35).

Our study revealed that cells expressing mutant RAS isoforms exhibit differential sensitivity to effector inhibition in maintaining their transformed phenotype. In cells expressing mutant N- or KRAS, isoforms that are relatively poor activators of PI3K, anchorage-independent growth was inhibited at lower doses of either the PI3K or AKT inhibitor than the dose required to inhibit growth in cells expressing mutant HRAS (Fig. 5). The converse was also true: in cells expressing mutant HRAS, an isoform that poorly activates Raf, anchorage-independent growth was inhibited at lower doses of the MEK inhibitor than the dose required in cells expressing mutant NRAS or KRAS. These data suggest that cells expressing mutant RAS isoforms are particularly sensitive to inhibition of RAS effectors that the oncogene poorly activates. Notably, this differential sensitivity to effector pathway inhibition was only observed in anchorage-independent growth assays, not in assays assessing anchorage-dependent (2D) growth, demonstrating that the appropriate culture system must be use to tease apart these drug sensitivities. Multiple studies have shown that *KRAS*-mutant cancer cell lines show a range of KRAS dependency for survival in 2D culture (44–48). However, many of these “KRAS-independent” cell lines still require KRAS for anchorage-independent growth (49–52). This finding suggests that we must take care in choosing the appropriate culture system to identify and test novel therapeutic targets to treat *RAS* mutant tumors, and that anchorage-independent 3D growth screens should be used to supplement current 2D screening efforts (50).

How are wild-type RAS isoforms activated in the context of mutant RAS?

Wild-type RAS isoforms cooperate with oncogenic RAS mutants to promote downstream effector activation and cell proliferation; however, the mechanistic underpinnings of this cooperation are unclear, as previous reports have shown two interconnected mechanisms of wild-type RAS activation in cells expressing mutant RAS. Both mechanisms involve RASGEFs as the direct activators of wild-type RAS, which raises the question: which mechanism underlies RASGEF-dependent wild-type RAS activation in the context of mutant RAS? For the first model, studies have shown that RTK-dependent activation of wild-type RAS acts in an interconnected network with basal mutant RAS^{GTP} signaling to promote G2 checkpoint integrity (53) and proliferation of *RAS* mutant cancer cells (11). Our data here support this model, and suggest that in cells expressing mutant RAS, robust RTK-dependent PI3K/AKT signaling is dependent on SOS2 (Fig. 4), and this RTK-SOS2-AKT signaling is important for transformation driven by KRAS, but not HRAS. Alternatively, for the second model, crystallographic studies of the RAS:SOS1 complexes show that SOS1 contains an allosteric RAS^{GTP} binding site, distinct from its catalytic RASGEF domain, that relieves SOS1 autoinhibition when occupied (16). This allosteric binding of RAS^{GTP} to SOS1 sets up a potential RAS^{GTP}-SOS1-RAS positive feedback loop that can potentiate EGF signaling to downstream effectors (54), support prolonged T-cell and B-cell receptor-dependent RAS/ERK activation (28, 55), and promote proliferation of *KRAS* mutant cancer cells (17). Our data show that wild-type RAS is activated in cells expressing mutant KRAS independently of RTK signaling and SOS2 expression, suggesting that a SOS1-dependent positive feedback loop plays a role in basal mutant RAS signaling to wild-type RAS (Fig. 3F).

What is the mechanism underlying the different contributions of SOS1 and SOS2 to wild-type RAS activation in RAS mutant tumors? SOS1 and SOS2 both interact with Grb2 via their proline-rich regions, where their sequences diverge. SOS2 has a much higher affinity for Grb2 than SOS1 does (56). Additionally, SOS1 is subject to ERK-dependent negative feedback phosphorylation that can regulate either dissociation of the Grb2/SOS1 complex or release of this complex from the EGFR (57–59), and this ERK-dependent feedback phosphorylation does not occur on SOS2 (60). These properties potentially make SOS2 a more suitable candidate for RTK-Grb2-dependent signaling in the presence of oncogenic RAS, where basal ERK signaling might phosphorylate SOS1 and cause its dissociation from receptor complexes. In contrast, the proline-rich region of SOS1 is not required for RAS^{GTP}-SOS1-RAS feedback signaling (61), and may inhibit engagement of the SOS1 allosteric site by RAS^{GTP} (62). However, the mechanism by which the proline-rich region of SOS1 regulates engagement of the allosteric site, and whether ERK-dependent phosphorylation of the SOS1 would inhibit or potentiate allosteric site engagement, remains to be tested.

Together, these findings may help explain why *Sos2* deletion has a differential effect on RAS-isoform driven transformation. We found that cells expressing any of the three mutant RAS isoforms are reliant on *Sos2* expression for maximal RTK-stimulated AKT phosphorylation (Fig. 4). However, since mutant KRAS is a relatively weak activator of PI3K compared to HRAS, it was more reliant on this RTK-SOS2-AKT signaling pathway to supplement its basal PI3K activation, and thus *Sos2* deletion had a more profound effect on mutant KRAS-driven transformation compared to HRAS (Fig. 1). A similar argument may explain why *Sos2* deletion preferentially affected transformation, but not proliferation, in cells expressing mutated KRAS. While the requirement for *Sos2* to promote KRAS-driven transformation depends on its supplementing the relatively weak PI3K activation by mutant KRAS, proliferation predominantly depends on ERK signaling, which is not defective in either primary $Sos2^{-/-}$ MEFs (18) or immortalized $Sos2^{-/-}$ MEFs expressing oncogenic RAS (Fig. 1B and 4).

The importance of PI3K signaling in KRAS tumors is widely established (63), as is the efficacy of combined MEK and PI3K inhibition in blocking KRAS-driven transformation, since inhibiting either pathway alone leads to activation of the other through relief of negative feedback (64, 65). Unfortunately, this treatment strategy has a high risk of toxicity, since the Raf/MEK/ERK and PI3K/AKT pathways are both key players in normal cell function. To avoid this toxicity, many studies have investigated the efficacy of blocking the PI3K pathway indirectly, or finding other pathways that synergize with MEK or PI3K inhibition (35, 66). For example, Ebi et al (35) show that PI3K signaling is downstream of IGFR in *KRAS*-mutant colon cancer cells, and that IGFR inhibition can indirectly block PI3K signaling. They also show that this indirect block coordinates with MEK inhibition to limit mutant tumor growth and promote apoptosis to the same extent as direct PI3K inhibition. When we compared the effects of *SOS2* deletion in combination with either PI3K inhibition (buparlisib) or MEK inhibition (trametinib) (Fig. 8), we found that *SOS2* deletion had the same effect as an intermediate dose of buparlisib when combined with trametinib. Coupled with the decrease in AKT phosphorylation we observed in the absence of SOS2, our findings point to SOS2 as an alternate target to indirectly block RTK-mediated PI3K signaling in KRAS-mutant cancer cells. SOS2 inhibition may be more broadly applicable

than inhibition of individual RTKs, since different RTKs are predominant in different types of KRAS-mutant cancers. Additionally, SOS2 is not necessary for development and normal adult cell function in the presence of SOS1 (67–69), so inhibition of SOS2 may have lower toxicity in non-tumor cells than inhibition of PI3K or RTKs. Overall, our findings point to a more complex role of RASGEF signaling in discriminating the effects of RAS isoform-driven transformation than has previously been appreciated and underline the importance of comprehensive examinations of the role of each RASGEF in RAS-driven transformation across RAS isoforms. In addition, our findings suggest that SOS2 inhibition should be pursued as a potential therapeutic option in KRAS-driven cancers.

Materials and Methods

Cell culture.

MEFs were maintained in Dulbecco's modified Eagle's medium (DMEM) and YAPC and H358 cells were maintained in Roswell Park Memorial Institute medium (RPMI), each supplemented with 10% fetal bovine serum, 2 mM l-glutamine, 0.1 mM minimum essential medium with nonessential amino acids, and 1% penicillin-streptomycin.

RAS construct cloning.

HA-HRAS^{G12V} was PCR amplified from pBabePuro and cloned into EcoRI/BamHI digested pCDH-CMV-MCS-EF1-Puro (System Biosciences) using the GeneArt Seamless Cloning and Assembly Kit (Invitrogen). To clone in wild-type KRAS and wild-type NRAS, pCDH-HA-HRAS^{G12V} was digest with BamHI/NotI to remove HRAS but maintain the HA tag, and wild-type KRAS or NRAS were PCR amplified and cloned in using GeneArt. Oncogenic point mutations (NRAS^{G12V} and KRAS (G12C, G12D, G12V, G13D, Q61L, and Q61R)) were then introduced by site-directed mutagenesis. To produce V5-tagged wild-type HRAS, Hs.HRAS (attL1-attL2 clone R999-E10) was cloned into pDest-658 (Blasticidin-resistant, attR4-attR2 lentiviral vector), along with the CMV51p promotor (C453–04, attL4-attL5 sites) and the V5 tag (C514-E24, attR5-attR1 sites) by Gateway Cloning (Invitrogen). All gateway clones were gifts from Dominic Esposito (RAS Project, Frederick National Laboratory).

SOS2 construct cloning.

Hs.SOS2 (attL1-attL2 clone 777-E319) was cloned into pDest-658 (Blasticidin-resistant, attR4-attR2 lentiviral vector) along with one of 5 different promoters (attL4-attR1 clones C413-E15 EF1p, C413-E33 UbCp, C413-E21 PGKp, C413-E34 mCMVp, C413-E26 SV40p) by Gateway Cloning (Invitrogen). All gateway clones were gifts from Dominic Esposito (RAS Project, Frederick National Laboratory). SOS2 W727E and F927A point mutations were introduced by site-directed mutagenesis of the wild-type SOS2 entry clone.

Production of recombinant lentiviruses.

Lentiviruses were produced by co-transfecting MISSION lentiviral packaging mix (Sigma) into 293T cells using calcium phosphate. Ecotropic p110α retrovirus was produced by calcium phosphate transfection of pBabePuro (p110α ^{H1047}) into Phoenix-Eco cells. At 48 to 72 h post-transfection, viral supernatants were collected and filtered. Viral supernatants

were then either stored at −80°C or used immediately to infect cells in combination with polybrene at 8 μg/mL. MEFs were selected with 4 μg/mL Puromycin (Invitrogen) or 2.5 μg/mL Blasticidin (Invitrogen). YAPC and H358 cells were selected with 6 μg/mL Puromycin.

Generation of cell lines.

Nonimmortalized MEFs were generated from 13.5-day *Sos1*$^{f/f}$ and *Sos1*$^{f/f}$*Sos2*$^{-/-}$ embryos using a previously described protocol. Cells were maintained in culture according to a 3T6 protocol until immortalized populations of cells emerged (21, 22).

Cell lysis and Western blot analysis.

For whole cell lysate (WCL) analysis, cells were either lysed while cycling or starved overnight prior to stimulation with 100 ng/mL EGF for the indicated times. Cells were then lysed in RIPA buffer (1% NP-40, 0.1% SDS, 0.1% Na-deoxycholate, 10% glycerol, 0.137 M NaCl, 20 mM Tris pH [8.0], protease and phosphatase inhibitor cocktails (Biotool)) for 20 minutes at 4°C and spun at 10,000 RPM for 10 minutes. Clarified lysates were boiled in SDS sample buffer containing 100 mM DTT for 10 minutes prior to Western blotting. Proteins were resolved by sodium dodecyl sulfate-polyacrylamide gel electrophoresis and transferred to nitrocellulose or PVDF membranes. Western blots were developed by multiplex Western blotting using anti-SOS1 (Santa Cruz sc-256; 1:500), anti-SOS2 (Santa Cruz sc-258; 1:500), anti-β-actin (Sigma AC-15; 1:5,000), anti-HA (Santa Cruz sc-805; 1:1000), anti-RAS (Cell Signaling 3965; 1:500), anti-V5 (Cell Signaling 13202; 1:1000), anti-pERK1/2 (Cell Signaling 4370; 1:2,000), anti-ERK1/2 (Cell Signaling 4696; 1:1000), anti-pAKT (Thr^{308} [Cell Signaling 2965; 1:1000] or Ser^{473} [Cell Signaling 4060; 1:1000]), anti-AKT (Cell Signaling 2920; 1:1000), anti-p110α PI3K (Cell Signaling 4249; 1:1000), anti-KRAS (Sigma WH0003845M1; 1:200), or anti-Tubulin (Cell Signaling; 1:1000) primary antibodies. Anti-mouse and anti-rabbit secondary antibodies conjugated to IRDye680 or IRDye800 (LI-COR; 1:10,000) were used to probe primary antibodies. Protein bands were detected and quantified by Western blotting with the Odyssey system (LI-COR). For quantification of SOS2 abundance, samples were normalized to either β-actin or tubulin. For quantification of pERK and pAKT, samples were normalized to a weighted average of β-actin, total ERK1/2, and total AKT (70).

RAS pull-downs.

For RAS pull-downs, cells were lysed on ice for 20 minutes in RAS-PD lysis buffer (1% NP-40, 50 mM Tris pH 7.5, 200 mM NaCl, 2.5 mM $MgCl_2$, protease and phosphatase inhibitor cocktails (Biotool)), and spun at 10,000 RPM for 10 minutes. GST-RBD bound to glutathione-sepharose beads was either prepared as previously described (71) or purchased (Millipore) and used to isolate RAS-GTP from lysates by rotating incubation for one hour at 4°C. Samples were washed four times in RAS-PD lysis buffer. All samples were boiled in 2× SDS sample buffer containing 100 mM DTT for 10 minutes prior to Western blotting.

Proliferation Studies.

For growth assays, 2×10^3 cells were seeded on cell culture-coated 96-well plates (CellTreat). Cells were lysed with CellTitre-Glo 2.0 Reagent (Promega), and luminescence was read using a GloMax Discover Plate Reader (Promega). Cell number was assessed 2 hours after plating to account for any discrepancies in plating, and then every 24 hours for 5 days. Data were analyzed as an increase in luminescence over Day 0. For inhibitor studies, 4×10^3 cells were seeded on cell-culture treated 96-well plates (CellTreat) to assess anchorage-dependent growth, and on ultra-low attachment 96-well plates (Corning Costar #3474) to assess anchorage-independent growth (49). On Day 4, cells were assessed using CellTitre-Glo 2.0 Reagent as described. Inhibitor data are plotted as a scaled dose-response curve for each cell line $(E_{drug} - E_{max})/(E_0 - E_{max})$, where E_{drug} is the effect of the drug at a given concentration, E_{max} is the maximal effect of the drug, and E_0 is the effect seen in the DMSO control (72, 73). Data were analyzed and IC_{50} and AUC values were calculated using Prism 7.

Transformation Studies:

Cells were seeded in 0.32% Nobel agar at 2×10^4 cells per 35-mm dish to assess anchorage-independent growth (soft agar assays) or at 10^5 cells per 6-cm dish to assess the loss of contact inhibition (focus forming assays). Soft agar colonies were counted 21–28 days after seeding; 10× images of focus forming assays were taken 14–21 days after seeding, and then the dishes were stained with 1% bromophenol blue (74). Stained focus forming assay dishes were scanned on a Biorad Chemidoc Imaging System and cell density was quantified using Image Lab software. For spheroid growth in ultra-low attachment 96-well round bottomed plates (Corning Costar #7007), cells were seeded at 500 cells per well with the indicated concentration of inhibitor or DMSO. Images were taken 16 hours after plating to assess initial spheroid size, and then 7 or 14 days later to assess the effects of drug treatment on spheroid growth (75). Spheroid size was quantified using ImageJ. In parallel plates, cell number was assessed at day 0, 7, and 14 using CellTitre-Glo 2.0 reagent.

sgRNA studies:

A non-targeting (NT) single guide RNA (sgRNA), a *KRAS*-targeted sgRNA, and the 16 potential *SOS2*-targeted sgRNAs were each cloned into pLentiCRISPRv2 as previously described (33). sgRNA sequences are given in supplemental table S1. Lentiviruses were produced as described above. 48 hours post-infection, cells were selected for 4 days in 6 μg/mL Puromycin, and then shifted into 3 μg/mL Puromycin for an additional 6 days. Ten days after selection, cells were analyzed for KRAS and SOS2 expression and plated for signaling and transformation assays.

Supplementary Material

Refer to Web version on PubMed Central for supplementary material.

Acknowledgments:

We thank Andrew L. Snow and Regina Day for helpful discussions throughout the project, and Regina Day for critical reading of the manuscript. We thank Dominic Esposito for Gateway Cloning reagents and helpful discussions throughout the project.

Funding: This work was supported by start-up funds from the Uniformed Services University of the Health Sciences (R.L.K.), a grant from the Congressionally Directed Medical Research Program to R.L.K. (LC160222), and the Intramural Research Program of the CCR, NCI, NIH (J.L. and D.K.M.).

References

1. Bivona TG et al., PKC regulates a farnesyl-electrostatic switch on K-Ras that promotes its association with Bcl-XL on mitochondria and induces apoptosis. Mol Cell 21, 481–493 (2006). [PubMed: 16483930]
2. Steelman LS et al., Roles of the Ras/Raf/MEK/ERK pathway in leukemia therapy. Leukemia 25, 1080–1094 (2011). [PubMed: 21494257]
3. Diaz R et al., The N-ras proto-oncogene can suppress the malignant phenotype in the presence or absence of its oncogene. Cancer Res 62, 4514–4518 (2002). [PubMed: 12154063]
4. Li J et al., LOH of chromosome 12p correlates with Kras2 mutation in non-small cell lung cancer. Oncogene 22, 1243–1246 (2003). [PubMed: 12606951]
5. Guerrero I, Villasante A, Corces V, Pellicer A, Loss of the normal N-ras allele in a mouse thymic lymphoma induced by a chemical carcinogen. Proc Natl Acad Sci U S A 82, 7810–7814 (1985). [PubMed: 3865197]
6. Diaz R et al., Inhibition of Ras oncogenic activity by Ras protooncogenes. Int J Cancer 113, 241–248 (2005). [PubMed: 15386411]
7. To MD et al., A functional switch from lung cancer resistance to susceptibility at the Pas1 locus in Kras2LA2 mice. Nat Genet 38, 926–930 (2006). [PubMed: 16823377]
8. Zhang Z et al., Wildtype Kras2 can inhibit lung carcinogenesis in mice. Nat Genet 29, 25–33 (2001). [PubMed: 11528387]
9. Fotiadou PP, Takahashi C, Rajabi HN, Ewen ME, Wild-type NRas and KRas perform distinct functions during transformation. Mol Cell Biol 27, 6742–6755 (2007). [PubMed: 17636015]
10. Lim KH, Ancrile BB, Kashatus DF, Counter CM, Tumour maintenance is mediated by eNOS. Nature 452, 646–649 (2008). [PubMed: 18344980]
11. Young A, Lou D, McCormick F, Oncogenic and wild-type Ras play divergent roles in the regulation of mitogen-activated protein kinase signaling. Cancer Discov 3, 112–123 (2013). [PubMed: 23103856]
12. Zhou B, Der CJ, Cox AD, The role of wild type RAS isoforms in cancer. Semin Cell Dev Biol 58, 60–69 (2016). [PubMed: 27422332]
13. Castellano E, Santos E, Functional specificity of ras isoforms: so similar but so different. Genes Cancer 2, 216–231 (2011). [PubMed: 21779495]
14. Hamilton M, Wolfman A, Oncogenic Ha-Ras-dependent mitogen-activated protein kinase activity requires signaling through the epidermal growth factor receptor. J Biol Chem 273, 28155–28162 (1998). [PubMed: 9774435]
15. Bentley C et al., A requirement for wild-type Ras isoforms in mutant KRas-driven signalling and transformation. Biochem J 452, 313–320 (2013). [PubMed: 23496764]
16. Margarit SM et al., Structural evidence for feedback activation by Ras.GTP of the Ras-specific nucleotide exchange factor SOS. Cell 112, 685–695 (2003). [PubMed: 12628188]
17. Jeng HH, Taylor LJ, Bar-Sagi D, Sos-mediated cross-activation of wild-type Ras by oncogenic Ras is essential for tumorigenesis. Nat Commun 3, 1168 (2012). [PubMed: 23132018]
18. Liceras-Boillos P et al., Sos1 disruption impairs cellular proliferation and viability through an increase in mitochondrial oxidative stress in primary MEFs. Oncogene 35, 6389–6402 (2016). [PubMed: 27157612]

19. Land H, Parada LF, Weinberg RA, Tumorigenic conversion of primary embryo fibroblasts requires at least two cooperating oncogenes. Nature 304, 596–602 (1983). [PubMed: 6308472]
20. Newbold RF, Overell RW, Fibroblast immortality is a prerequisite for transformation by EJ c-Ha-ras oncogene. Nature 304, 648–651 (1983). [PubMed: 6877385]
21. Todaro GJ, Green H, Quantitative studies of the growth of mouse embryo cells in culture and their development into established lines. J Cell Biol 17, 299–313 (1963). [PubMed: 13985244]
22. Kortum RL et al., The molecular scaffold kinase suppressor of Ras 1 is a modifier of RasV12-induced and replicative senescence. Mol Cell Biol 26, 2202–2214 (2006). [PubMed: 16507997]
23. Cox AD, Fesik SW, Kimmelman AC, Luo J, Der CJ, Drugging the undruggable RAS: Mission possible? Nat Rev Drug Discov 13, 828–851 (2014). [PubMed: 25323927]
24. Haigis KM, KRAS Alleles: The Devil Is in the Detail. Trends Cancer 3, 686–697 (2017). [PubMed: 28958387]
25. Hunter JC et al., Biochemical and Structural Analysis of Common Cancer-Associated KRAS Mutations. Mol Cancer Res 13, 1325–1335 (2015). [PubMed: 26037647]
26. Shi T et al., Conservation of protein abundance patterns reveals the regulatory architecture of the EGFR-MAPK pathway. Sci Signal 9, rs6 (2016). [PubMed: 27405981]
27. Hall BE, Yang SS, Boriack-Sjodin PA, Kuriyan J, Bar-Sagi D, Structure-based mutagenesis reveals distinct functions for Ras switch 1 and switch 2 in Sos-catalyzed guanine nucleotide exchange. J Biol Chem 276, 27629–27637 (2001). [PubMed: 11333268]
28. Roose JP, Mollenauer M, Ho M, Kurosaki T, Weiss A, Unusual interplay of two types of Ras activators, RasGRP and SOS, establishes sensitive and robust Ras activation in lymphocytes. Mol Cell Biol 27, 2732–2745 (2007). [PubMed: 17283063]
29. Denley A, Kang S, Karst U, Vogt PK, Oncogenic signaling of class I PI3K isoforms. Oncogene 27, 2561–2574 (2008). [PubMed: 17998941]
30. Oda K et al., PIK3CA cooperates with other phosphatidylinositol 3'-kinase pathway mutations to effect oncogenic transformation. Cancer Res 68, 8127–8136 (2008). [PubMed: 18829572]
31. Li W, Zhu T, Guan KL, Transformation potential of Ras isoforms correlates with activation of phosphatidylinositol 3-kinase but not ERK. J Biol Chem 279, 37398–37406 (2004). [PubMed: 15210703]
32. Munoz DM et al., CRISPR Screens Provide a Comprehensive Assessment of Cancer Vulnerabilities but Generate False-Positive Hits for Highly Amplified Genomic Regions. Cancer Discov 6, 900–913 (2016). [PubMed: 27260157]
33. Sanjana NE, Shalem O, Zhang F, Improved vectors and genome-wide libraries for CRISPR screening. Nat Methods 11, 783–784 (2014). [PubMed: 25075903]
34. Janes MR et al., Targeting KRAS Mutant Cancers with a Covalent G12C-Specific Inhibitor. Cell 172, 578–589 e517 (2018). [PubMed: 29373830]
35. Ebi H et al., Receptor tyrosine kinases exert dominant control over PI3K signaling in human KRAS mutant colorectal cancers. J Clin Invest 121, 4311–4321 (2011). [PubMed: 21985784]
36. Engelman JA et al., Effective use of PI3K and MEK inhibitors to treat mutant Kras G12D and PIK3CA H1047R murine lung cancers. Nat Med 14, 1351–1356 (2008). [PubMed: 19029981]
37. Anderson GR et al., A Landscape of Therapeutic Cooperativity in KRAS Mutant Cancers Reveals Principles for Controlling Tumor Evolution. Cell Rep 20, 999–1015 (2017). [PubMed: 28746882]
38. Prior IA, Lewis PD, Mattos C, A comprehensive survey of Ras mutations in cancer. Cancer Res 72, 2457–2467 (2012). [PubMed: 22589270]
39. Stephen AG, Esposito D, Bagni RK, McCormick F, Dragging ras back in the ring. Cancer Cell 25, 272–281 (2014). [PubMed: 24651010]
40. Yan J, Roy S, Apolloni A, Lane A, Hancock JF, Ras isoforms vary in their ability to activate Raf-1 and phosphoinositide 3-kinase. J Biol Chem 273, 24052–24056 (1998). [PubMed: 9727023]
41. Voice JK, Klemke RL, Le A, Jackson JH, Four human ras homologs differ in their abilities to activate Raf-1, induce transformation, and stimulate cell motility. J Biol Chem 274, 17164–17170 (1999). [PubMed: 10358073]

42. Herrmann C, Martin GA, Wittinghofer A, Quantitative analysis of the complex between p21ras and the Ras-binding domain of the human Raf-1 protein kinase. J Biol Chem 270, 2901–2905 (1995). [PubMed: 7852367]
43. Maher J, Baker DA, Manning M, Dibb NJ, Roberts IA, Evidence for cell-specific differences in transformation by N-, H- and K-ras. Oncogene 11, 1639–1647 (1995). [PubMed: 7478589]
44. Balbin OA et al., Reconstructing targetable pathways in lung cancer by integrating diverse omics data. Nat Commun 4, 2617 (2013). [PubMed: 24135919]
45. Singh A et al., A gene expression signature associated with “K-Ras addiction” reveals regulators of EMT and tumor cell survival. Cancer Cell 15, 489–500 (2009). [PubMed: 19477428]
46. Singh A et al., TAK1 inhibition promotes apoptosis in KRAS-dependent colon cancers. Cell 148, 639–650 (2012). [PubMed: 22341439]
47. Scholl C et al., Synthetic lethal interaction between oncogenic KRAS dependency and STK33 suppression in human cancer cells. Cell 137, 821–834 (2009). [PubMed: 19490892]
48. Lamba S et al., RAF suppression synergizes with MEK inhibition in KRAS mutant cancer cells. Cell Rep 8, 1475–1483 (2014). [PubMed: 25199829]
49. Fujita-Sato S et al., Enhanced MET Translation and Signaling Sustains K-Ras-Driven Proliferation under Anchorage-Independent Growth Conditions. Cancer Res 75, 2851–2862 (2015). [PubMed: 25977330]
50. Rotem A et al., Alternative to the soft-agar assay that permits high-throughput drug and genetic screens for cellular transformation. Proc Natl Acad Sci U S A 112, 5708–5713 (2015). [PubMed: 25902495]
51. Zhang Z, Jiang G, Yang F, Wang J, Knockdown of mutant K-ras expression by adenovirus-mediated siRNA inhibits the in vitro and in vivo growth of lung cancer cells. Cancer Biol Ther 5, 1481–1486 (2006). [PubMed: 17172815]
52. McCormick F, KRAS as a Therapeutic Target. Clin Cancer Res 21, 1797–1801 (2015). [PubMed: 25878360]
53. Grabocka E et al., Wild-type H- and N-Ras promote mutant K-Ras-driven tumorigenesis by modulating the DNA damage response. Cancer Cell 25, 243–256 (2014). [PubMed: 24525237]
54. Boykevisch S et al., Regulation of ras signaling dynamics by Sos-mediated positive feedback. Curr Biol 16, 2173–2179 (2006). [PubMed: 17084704]
55. Das J et al., Digital signaling and hysteresis characterize ras activation in lymphoid cells. Cell 136, 337–351 (2009). [PubMed: 19167334]
56. Yang SS, Van Aelst L, Bar-Sagi D, Differential interactions of human Sos1 and Sos2 with Grb2. J Biol Chem 270, 18212–18215 (1995). [PubMed: 7629138]
57. Langlois WJ, Sasaoka T, Saltiel AR, Olefsky JM, Negative feedback regulation and desensitization of insulin- and epidermal growth factor-stimulated p21ras activation. J Biol Chem 270, 25320–25323 (1995). [PubMed: 7592690]
58. Kamioka Y, Yasuda S, Fujita Y, Aoki K, Matsuda M, Multiple decisive phosphorylation sites for the negative feedback regulation of SOS1 via ERK. J Biol Chem 285, 33540–33548 (2010). [PubMed: 20724475]
59. Dong C, Waters SB, Holt KH, Pessin JE, SOS phosphorylation and disassociation of the Grb2-SOS complex by the ERK and JNK signaling pathways. J Biol Chem 271, 6328–6332 (1996). [PubMed: 8626428]
60. Corbalan-Garcia S, Yang SS, Degenhardt KR, Bar-Sagi D, Identification of the mitogen-activated protein kinase phosphorylation sites on human Sos1 that regulate interaction with Grb2. Mol Cell Biol 16, 5674–5682 (1996). [PubMed: 8816480]
61. Christensen SM et al., One-way membrane trafficking of SOS in receptor-triggered Ras activation. Nat Struct Mol Biol 23, 838–846 (2016). [PubMed: 27501536]
62. Lee YK et al., Mechanism of SOS PR-domain autoinhibition revealed by single-molecule assays on native protein from lysate. Nat Commun 8, 15061 (2017). [PubMed: 28452363]
63. Krygowska AA, Castellano E, PI3K: A Crucial Piece in the RAS Signaling Puzzle. Cold Spring Harbor Perspectives in Medicine, (2017).

64. Sos ML et al., Identifying genotype-dependent efficacy of single and combined PI3K- and MAPK-pathway inhibition in cancer. Proc Natl Acad Sci U S A 106, 18351–18356 (2009). [PubMed: 19805051]

65. Engelman JA et al., Effective Use of PI3K and MEK Inhibitors to Treat Mutant K-Ras G12D and PIK3CA H1047R Murine Lung Cancers. Nature medicine 14, 1351–1356 (2008).

66. Anderson GR et al., A Landscape of Therapeutic Cooperativity in KRAS Mutant Cancers Reveals Principles for Controlling Tumor Evolution. Cell Reports 20, 999–1015 (2017). [PubMed: 28746882]

67. Esteban LM et al., Ras-Guanine Nucleotide Exchange Factor Sos2 Is Dispensable for Mouse Growth and Development. Molecular and Cellular Biology 20, 6410–6413 (2000). [PubMed: 10938118]

68. Baltanás FC et al., Functional Redundancy of Sos1 and Sos2 for Lymphopoiesis and Organismal Homeostasis and Survival. Molecular and Cellular Biology 33, 4562–4578 (2013). [PubMed: 24043312]

69. Kortum RL et al., Deconstructing Ras Signaling in the Thymus. Molecular and Cellular Biology 32, 2748–2759 (2012). [PubMed: 22586275]

70. Janes KA, An analysis of critical factors for quantitative immunoblotting. Sci Signal 8, rs2 (2015). [PubMed: 25852189]

71. Castro AF, Rebhun JF, Quilliam LA, Measuring Ras-family GTP levels in vivo--running hot and cold. Methods 37, 190–196 (2005). [PubMed: 16289967]

72. Stephenson RP, A modification of receptor theory. Br J Pharmacol Chemother 11, 379–393 (1956). [PubMed: 13383117]

73. Harris LA et al., An unbiased metric of antiproliferative drug effect in vitro. Nat Methods 13, 497–500 (2016). [PubMed: 27135974]

74. Kortum RL, Lewis RE, The molecular scaffold KSR1 regulates the proliferative and oncogenic potential of cells. Mol Cell Biol 24, 4407–4416 (2004). [PubMed: 15121859]

75. Vinci M et al., Advances in establishment and analysis of three-dimensional tumor spheroid-based functional assays for target validation and drug evaluation. BMC Biol 10, 29 (2012). [PubMed: 22439642]

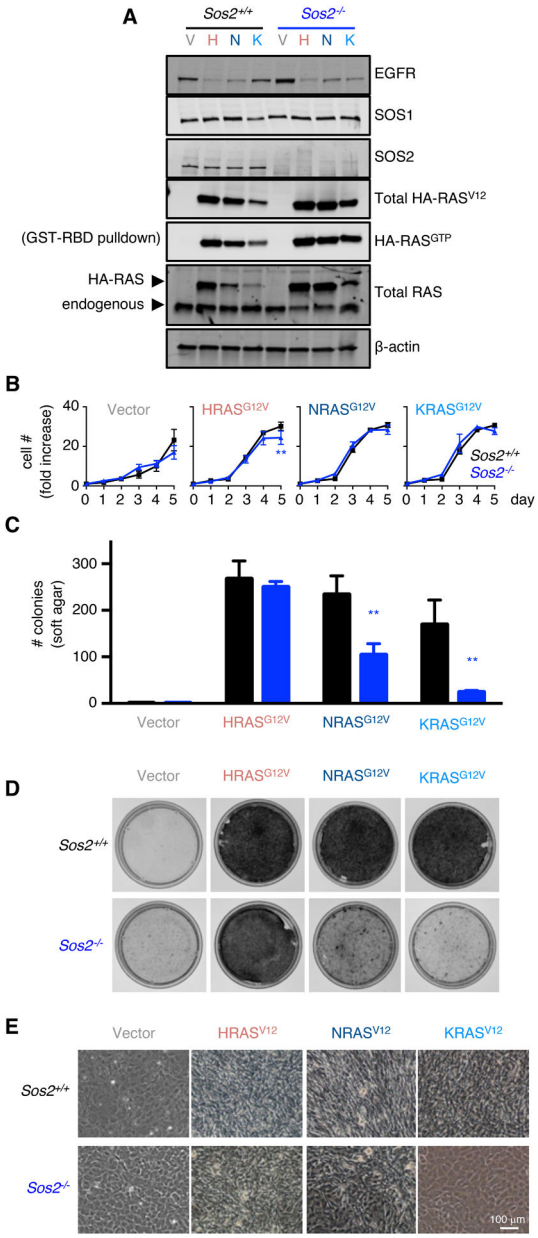

Fig. 1. Oncogenic mutant RAS isoforms show a hierarchical requirement for SOS2 to drive transformation in MEFs.

(A) *Sos2*$^{+/+}$ and *Sos2*$^{-/-}$ MEFs were transduced with lentiviruses expressing either empty vector (V) or the indicated HA-tagged mutant RAS isoform (H, N, and K: HRAS^{G12V}, NRAS^{G12V}, and KRAS^{G12V}, respectively). Whole cell lysates (WCLs) were analyzed by Western blotting with antibodies specific for EGFR, SOS1, SOS2, HA (for RAS^{G12V}), total RAS, or β-actin to assess total protein. GST-RAS binding domain pulldowns were analyzed by Western blotting with an antibody specific for the HA epitope to assess activation of mutant HA-RAS^{G12V}. Blots are representative of three independent experiments. **(B-D)** *Sos2*$^{+/+}$ and *Sos2*$^{-/-}$ MEFs expressing the indicated mutant RAS isoform were assessed for (B) proliferation in 2D culture plates, (C) colony growth in soft agar to assess anchorage-independent growth, and (D) loss of contact inhibition as assessed by a focus forming assay.

Data are mean ± SD from three independent experiments. ** P<0.01 by ANOVA using the Tukey's method to correct for multiple comparisons. **(E)** 10× images of post-confluent MEFs from **D**. Images are representative from three independent experiments. See also fig. S1 for an overlay of the proliferation curves in **B.**

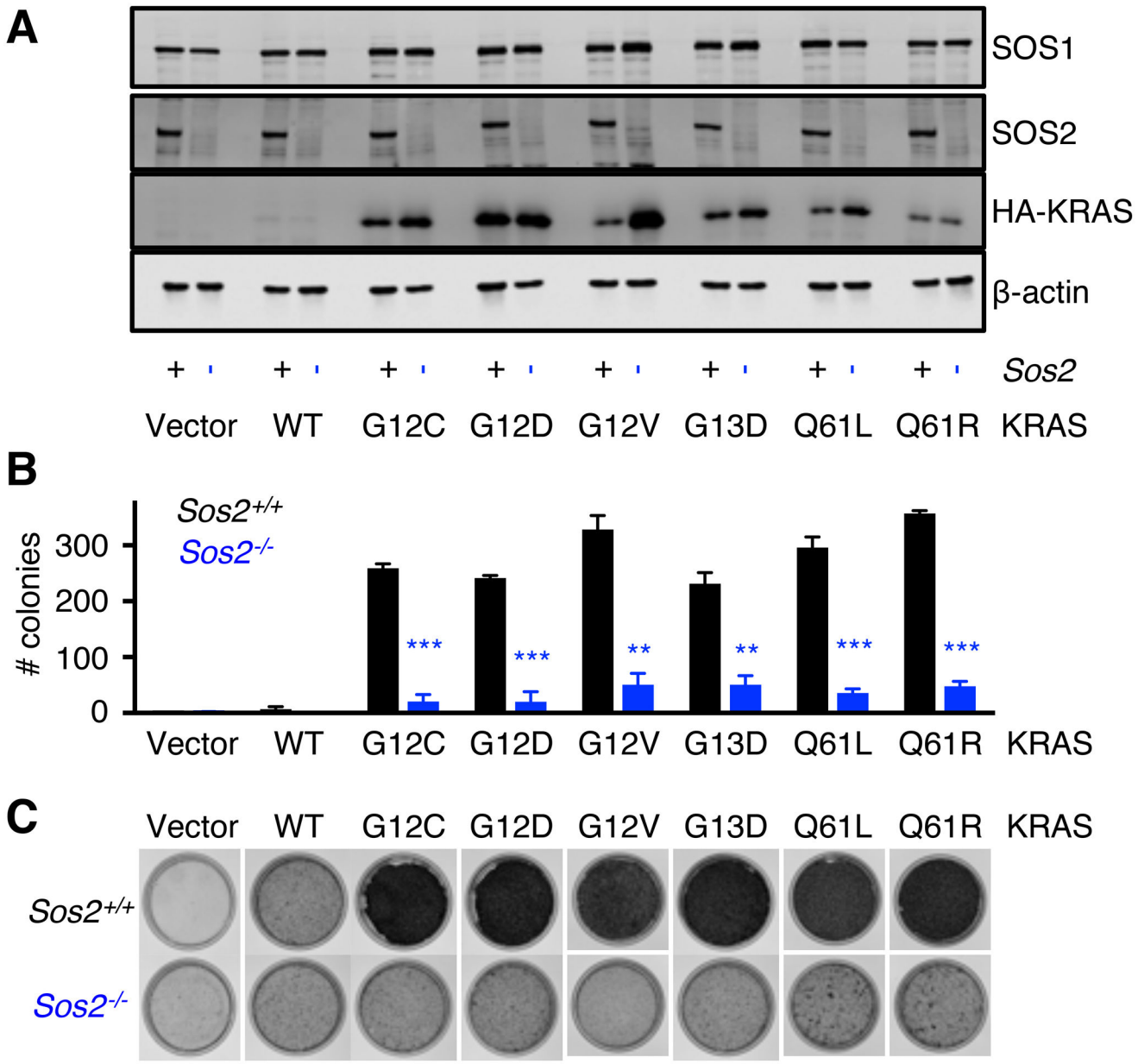

Fig. 2. Sos2 is required for mutant KRAS driven transformation in MEFs.

(A) *Sos2*$^{+/+}$ (+) and *Sos2*$^{-/-}$ (–) MEFs were transduced with lentiviruses expressing either empty vector (V), wild-type KRAS, or the indicated HA-tagged mutant KRAS constructs. Whole cell lysates (WCLs) were analyzed by Western blotting with antibodies specific for SOS2, HA (KRAS), or β-actin. Blots are representative of three independent experiments. **(B-C)** *Sos2*$^{+/+}$ and *Sos2*$^{-/-}$ MEFs expressing the indicated KRAS constructs were assessed for **(B)** colony growth in soft agar to assess anchorage independent growth, and **(C)** loss of contact inhibition as assessed by focus forming assay. Data are mean ± SD from three independent experiments. Statistical significance was determined by ANOVA using the Tukey's method to correct for multiple comparisons. ** P<0.01; *** P<0.001.

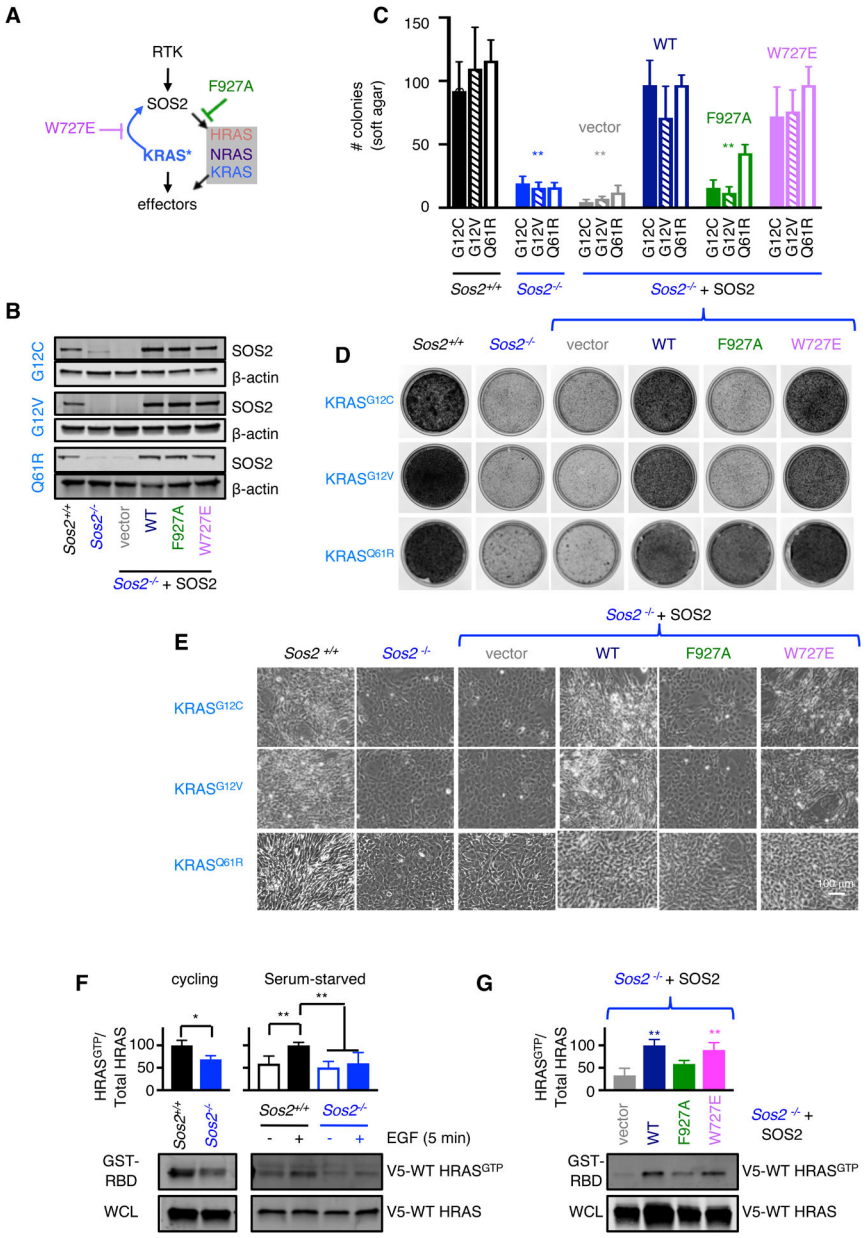

Fig. 3. Sos2 RASGEF activity contributes to KRAS4B–driven transformation.

(A) Schematic showing potential routes of SOS2-dependent wild-type RAS activation in the presence of mutant KRAS. SOS2 point mutants block either RASGEF activity (F927A) or putative allosteric SOS2 activation by KRAS (W727E). **(B)** *Sos2*$^{-/-}$ MEFs expressing KRAS^{G12C}, KRAS^{G12V}, or KRAS^{Q61R} were transduced with lentiviruses expressing either empty vector (V), wild-type SOS2, RASGEF-dead (F927A) SOS2, or feedback-defective (W727E) SOS2. Whole cell lysates (WCLs) were analyzed by Western blotting with antibodies specific for SOS2 or β-actin. Blots are representative of three independent experiments. **(C-D)** *Sos2*$^{+/+}$ *MEFs*, *Sos2*$^{-/-}$ MEFs, or *Sos2*$^{-/-}$ MEFs expressing the indicated SOS2 constructs along with either KRAS^{G12C} (closed), KRAS^{G12V} (hashed), or KRAS^{Q61R} (open) were assessed for **(C)** colony growth in soft agar to assess anchorage

independent growth, and **(D)** loss of contact inhibition by focus forming assay. Data are mean ± SD from three independent experiments. Statistical significance was determined by ANOVA using the Tukey's method to correct for multiple comparisons. For **C**, ** P<0.01 versus *Sos2*$^{+/+}$ and WT. **(E)** 10 × images of post-confluent MEFs from **D**. Images are representative of 3 independent experiments. **(F-G)** Western blotting for activated V5-HRAS from GST-RBD pulldowns (middle, quantified above) or for total V5-HRAS from WCLs (below) from **(F)** *Sos2*$^{+/+}$ or *Sos2*$^{-/-}$ MEFs expressing HA-KRAS^{G12C} and V5-wild-type HRAS in either actively cycling cells (left) or cells serum starved overnight and then lysed or stimulated with 100 μg/mL EGF for 5 minutes (right) or **(G)** *Sos2*$^{-/-}$ MEFs expressing HA-KRAS^{G12C}, V5-wild-type HRAS, and the indicated SOS2 construct. Data are mean ± SD from three independent experiments. Blots are representative of three independent experiments. Statistical significance was determined by ANOVA using the Tukey's method to correct for multiple comparisons. For **F**, * P<0.05; ** P<0.01. For **G**, **P<0.01 versus vector and SOS2^{F927A}.

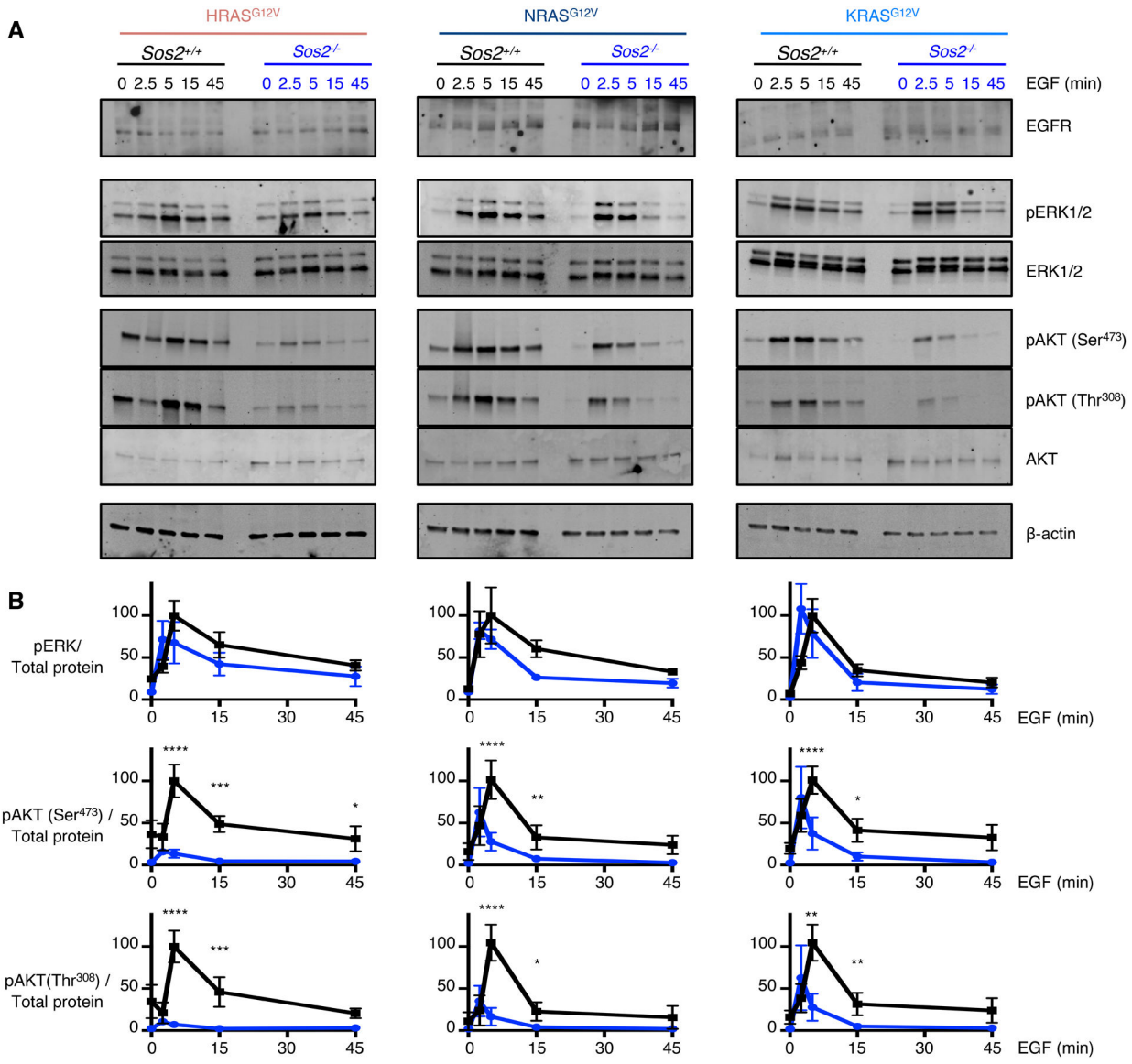

Fig. 4: SOS2 is required for optimal RTK−dependent AKT phosphorylation in cells expressing mutant RAS.

Sos2$^{+/+}$ and *Sos2*$^{-/-}$ MEFs expressing the indicated mutant RAS isoforms were placed in serum-free media overnight, and then stimulated with 100 μg/mL EGF for the indicated times. **(A)** WCLs were analyzed by multiplex Western blotting for pERK1/2, ERK1/2, pAKT (Ser^{473}), pAKT (Thr^{308}), AKT, and β-actin on a LI-COR Odyssey machine. Blots are representative of three independent experiments. **(B)** Quantification of pERK1/2, pAKT (Ser^{473}), and pAKT (Thr^{308}) levels versus a weighted average of total proteins (ERK1/2, AKT, and β-actin). Data are mean ± SD from three independent experiments. Statistical significance was determined by ANOVA using the Tukey's method to correct for multiple comparisons. * P<0.05; ** P<0.01; *** P<0.001; **** P<0.0001.

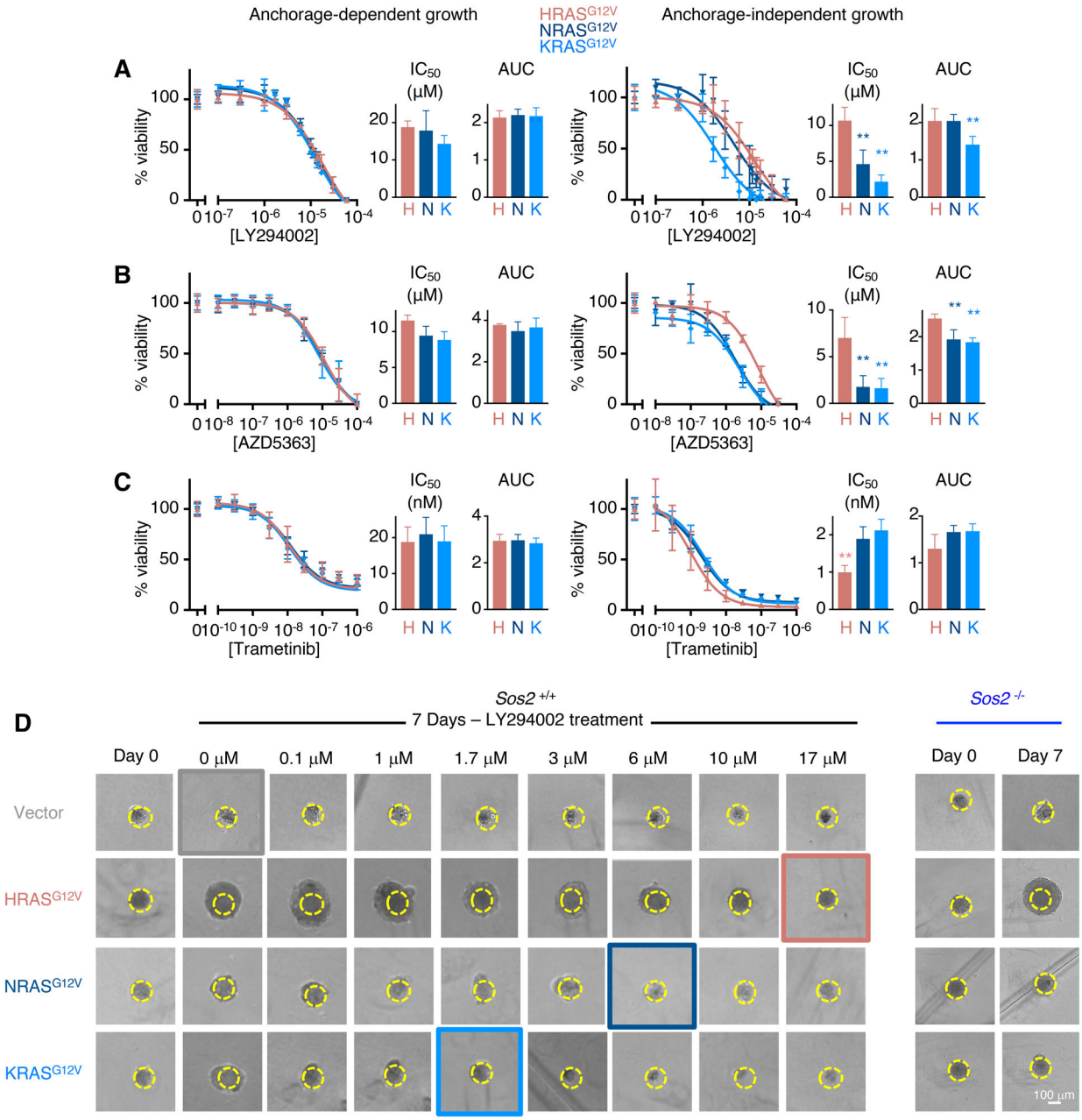

Fig. 5: Mutant RAS isoforms show a hierarchical requirement for PI3K signaling to drive transformation in MEFs.

Sos2$^{+/+}$ MEFs expressing the indicated mutant RAS isoforms were seeded onto either tissue-culture treated 96-well plates to assess anchorage-dependent growth or low-attachment 96-well plates to assess anchorage-independent growth. Cells were treated with the indicated concentrations of **(A)** the PI3K inhibitor LY294002, **(B)** the AKT inhibitor AZD5363, or **(C)** the MEK1/2 inhibitor trametinib for four days, and cell number was assessed. Data are expressed relative to vehicle-treated controls and are expressed as mean ± SD four independent experiments. IC_{50} values and AUC measurements are shown. Statistical significance was determined by ANOVA using the Tukey's method to correct for

multiple comparisons. ** P<0.01 versus $HRAS^{G12V}$. $HRAS^{G12V}$ (salmon triangles), $NRAS^{G12V}$ (purple inverted triangles), $KRAS^{G12V}$ (blue diamonds). **(D)** *Sos2*$^{+/+}$ MEFs expressing the indicated mutant RAS isoforms were seeded in low-attachment 96-well round-bottomed plates and treated with the indicated concentrations of the PI3K inhibitor LY294002 to assess the effects of PI3K inhibition on RAS-induced cancer spheroid formation (left). *Sos2*$^{-/-}$ MEFs expressing the indicated mutant RAS isoforms were seeded in parallel and left untreated for comparison (right). Images of spheroids were taken 16 hours after plating (Day 0) and again seven days later. Data are representative of three independent experiments. The outlined image for each cell line represents the LY294002 concentration where cancer spheroid size did not increase relative to Day 0. Images are representative of three independent experiments. See fig. S4 for inhibition of downstream protein phosphorylation by specific inhibitors, and fig. S5 for quantification of spheroid growth between *Sos2*$^{+/+}$ and *Sos2*$^{-/-}$ MEFs expressing mutant RAS.

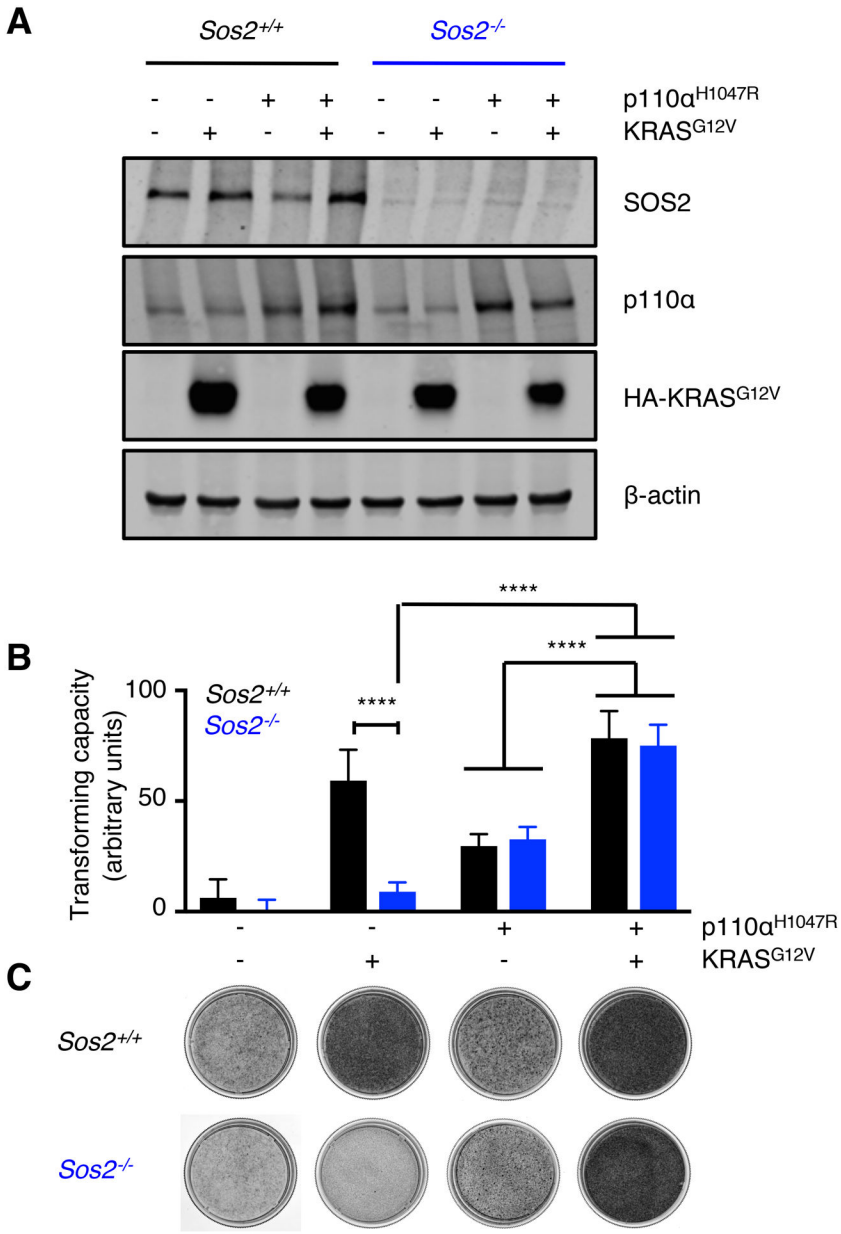

Fig. 6: Activated PI3K (p110α) cooperates with mutant KRAS4B to transform *Sos2*$^{-/-}$ MEFs.

(A) *Sos2*$^{+/+}$ and *Sos2*$^{-/-}$ MEFs were transduced with lentiviruses expressing KRAS^{G12V} +/− p110α^{H1047R}. Whole cell lysates (WCLs) were analyzed by Western blotting with antibodies specific for SOS2, p110α, HA (KRAS^{G12V}), or β-actin. Blots are representative of three independent experiments. **(B)** *Sos2*$^{+/+}$ and *Sos2*$^{-/-}$ MEFs expressing KRAS^{G12V} +/− p110α^{H1047R} were assessed for loss of contact inhibition by focus forming assay (stained dishes below, quantified above). Images are representative from three independent experiments. See fig. S6 for 10 × images of cells from **B.**

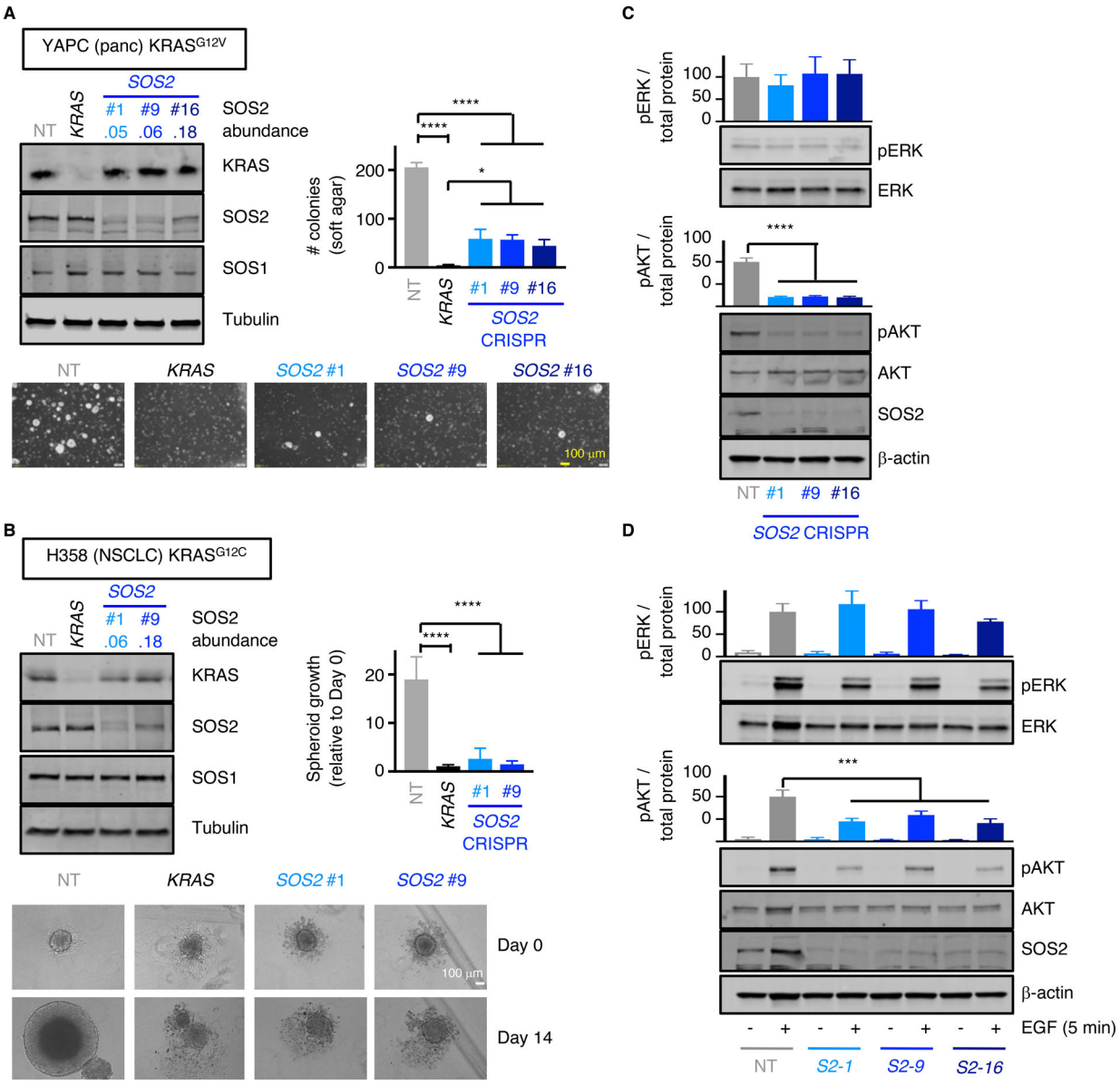

Fig. 7: SOS2 is required for transformation of *KRAS* mutated tumor cells.

(A) YAPC pancreatic cancer cells (harboring a KRAS^{G12V} mutation) were transduced with lentiviruses expressing Cas9 and either a non-targeting sgRNA (NT), an sgRNA targeting *KRAS*, or one of three different sgRNAs targeting *SOS2*. WCLs were analyzed by Western blotting with antibodies specific for KRAS, SOS2, SOS1, or tubulin (left). The SOS2 protein abundance relative to the NT sgRNA control in the *SOS2* CRISPR samples is given. Cells were assessed for colony growth in soft agar 21 days after plating to assess anchorage independent growth (right), and 10× images showing transformed colonies growing in soft agar were taken (bottom). Data are mean ± SD from three independent experiments. Blots and images are representative of 3 independent experiments. Statistical significance was determined by ANOVA using the Tukey's method to correct for multiple comparisons. * P<0.05; *** P<0.001; **** P<0.0001.

(B) H358 NSCLC cells (harboring a $KRAS^{G12C}$ mutation) were transduced with lentiviruses expressing Cas9 and either a non-targeting sgRNA (NT), an sgRNA targeting *KRAS*, or one of two different sgRNAs targeting *SOS2*. WCLs were analyzed by Western blotting with antibodies specific for KRAS, SOS2, SOS1, or tubulin (left). The SOS2 protein abundance relative to the NT sgRNA control in the *SOS2* CRISPR samples is given. Cells were assessed for anchorage independent growth by cancer spheroid assay (right), and cancer spheroid growth 16 hours after plating (day 0) or 14 days later (10× images below). Data are mean ± SD from three independent experiments. Blots and images are representative of 3 independent experiments. Statistical significance was determined by ANOVA using the Tukey's method to correct for multiple comparisons. * P<0.05; *** P<0.001; **** P<0.0001. **(C-D)** YAPC cells from **A** were either lysed actively cycling **(C)** or starved overnight and then stimulated with EGF 100 ng/mL for 5 minutes **(D)** prior to lysis. Multiplex Western blotting for pERK1/2, ERK1/2, pAKT (Ser^{473}), AKT, and β-actin was performed on a LI-COR Odyssey machine. Quantification of pERK1/2 and pAKT (Ser^{473}) levels versus a weighted average of total proteins (ERK1/2, AKT, and β-actin) are shown above. Data are mean ± SD from three independent experiments. Blots and images are representative of 3 independent experiments. Statistical significance was determined by ANOVA using the Tukey's method to correct for multiple comparisons. * P<0.05; *** P<0.001; **** P<0.0001.

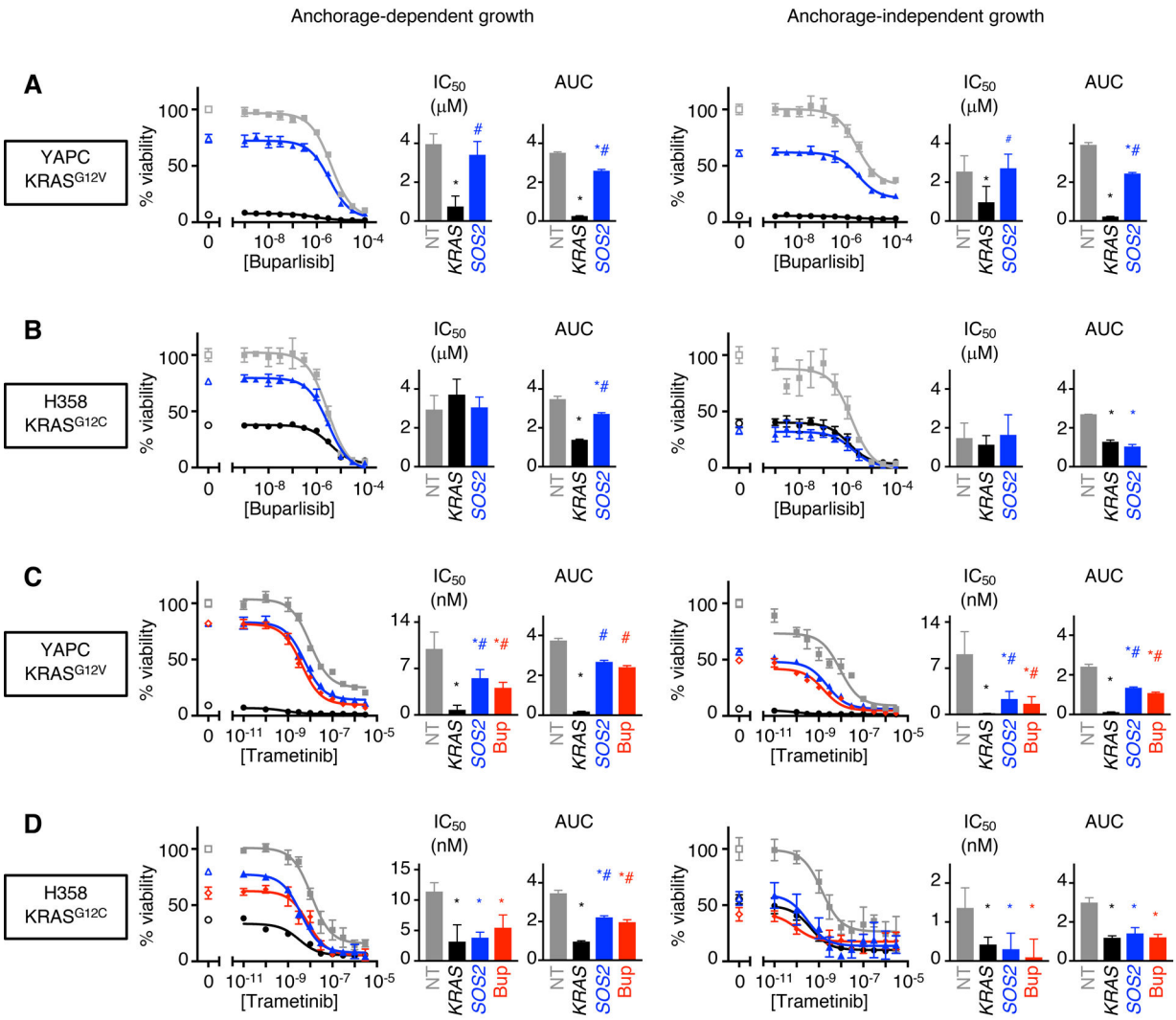

Fig. 8: *SOS2* deletion synergizes with MEK inhibition to inhibit transformation of *KRAS* mutant tumor cells.

(A-D) *KRAS* mutant YAPC pancreatic cancer cells **(A, C)** or H358 NSCLC cells **(B, D)** transduced with lentiviruses expressing Cas9 and either a non-targeting sgRNA (NT), an sgRNA targeting *KRAS*, or an sgRNAs targeting *SOS2* were seeded onto either tissue-culture treated 96-well plates to assess anchorage-dependent growth (left) or low-attachment 96-well plates to assess anchorage-independent growth (right). Cells were treated with the indicated concentrations of the PI3K inhibitor buparlisib **(A-B)** or the MEK1/2 inhibitor trametinib **(C-D)** for five days, and cell number was assessed. For **C-D**, NT cells were either treated with the indicated concentration of trametinib alone or in the presence of 100 ng/mL buparlisib. Data are expressed relative to vehicle-treated controls and are expressed as mean ± SD for three independent experiments. IC_{50} values and AUC measurements are shown. Statistical significance was determined by ANOVA using the Tukey's method to correct for multiple comparisons. * P<0.05 versus NT. # P<0.05 versus *KRAS* deletion. NT (grey

squares), *KRAS* deleted (black circles), *SOS2* deleted (blue triangles), NT + 100 ng/mL buparlisib (red diamonds).